ornl

OAK RIDGE NATIONAL LABORATORY

UNION CARBIDE

NUREG/CR-2900
ORNL-5876

Predicted Rates of Formation of Iodine Hydrolysis Species at pH Levels, Concentrations, and Temperatures Anticipated in LWR Accidents

J. T. Bell
M. H. Lietzke
D. A. Palmer

Prepared for the
U.S. Nuclear Regulatory Commission
Office of Nuclear Regulatory Research
Under Interagency Agreement 41 89 55 13 5

OPERATED BY
UNION CARBIDE CORPORATION
FOR THE UNITED STATES
DEPARTMENT OF ENERGY

Printed in the United States of America. Available from
National Technical Information Service
U.S. Department of Commerce
5285 Port Royal Road, Springfield, Virginia 22161

Available from

GPO Sales Program
Division of Technical Information and Document Control
U.S. Nuclear Regulatory Commission
Washington, D.C. 20555

NUREG/CR-2900
ORNL-5876
Dist. Category R3

Contract No. W-7405-eng-26

CHEMICAL TECHNOLOGY AND CHEMISTRY DIVISIONS

PREDICTED RATES OF FORMATION OF IODINE HYDROLYSIS SPECIES AT pH LEVELS, CONCENTRATIONS, AND TEMPERATURES ANTICIPATED IN LWR ACCIDENTS

J. T. Bell

Chemical Technology Division

M. H. Lietzke
D. A. Palmer

Chemistry Division

Manuscript Completed: August 1982
Date Published: October 1982

Prepared for the
U.S. Nuclear Regulatory Commission
Office of Nuclear Regulatory Research
Washington, D.C. 20555
Under Interagency Agreement 41 89 55 13 5
NRC FIN No. B0453

Prepared by the
OAK RIDGE NATIONAL LABORATORY
Oak Ridge, Tennessee 37830
operated by
UNION CARBIDE CORPORATION
for the
DEPARTMENT OF ENERGY

ABSTRACT

The literature was reviewed to define the kinetics for the reactions that follow dissolution of a molecular iodine source into water. Rate constants and rate expressions that had been determined for iodine reactions at temperatures below 60°C were extrapolated by various procedures to 125°C. Thus, a kinetic model was developed, and computer program IRATE was written to calculate the concentrations of aqueous iodine species as a function of time. The concentrations of the significant iodine species in aqueous solutions were calculated as a function of time to 10^9 s for six concentrations of total iodine that spanned the 10^{-9} to 10^{-3} g-atom/L range at 25, 60, 100, and 125°C, and with eight pH conditions that spanned the 3 to 11 range. Corresponding partition coefficients were calculated for selected conditions, with the assumption that only the I_2 and HOI species are volatile. The results are presented in the form of 35 figures, which contain a total of 93 plots.

CONTENTS

LIST OF FIGURES

Figure | Page

PREDICTED RATES OF FORMATION OF IODINE HYDROLYSIS SPECIES AT pH LEVELS, CONCENTRATIONS, AND TEMPERATURES ANTICIPATED IN LWR ACCIDENTS

J. T. Bell
M. H. Lietzke
D. A. Palmer

1. INTRODUCTION

In a previous report,[1] we reviewed the fundamental equilibrium chemistry of iodine hydrolysis and assessed that chemistry with respect to the conditions in light water reactor (LWR) accidents. The discussion included:

1. general information about iodine,
2. chemical conditions in an LWR accident,
3. reactions of iodine species in and with water,
4. the equilibrium distribution of iodine species in aqueous solution when the iodine source is molecular iodine,
5. equilibrium partitioning of iodine species between the aqueous system and its vapor,
6. a qualitative consideration of organic iodides.

The initial study did not consider the rates of the iodine reactions, namely, the species distribution before equilibrium is attained or the preequilibrium liquid-vapor distribution of iodine species. In the present study, we calculated the concentrations of the iodine species in aqueous solutions, and the associated partition coefficients, as a function of time for total iodine concentrations of 10^{-9} to 10^{-3} g-atom/L at temperatures of 25 to 125°C over the pH range of 4 to 11. The effects of initial iodide in retarding the I_2-H_2O reactions were also determined. Chemical reactions such as radiolysis, photolysis, and redox reactions with impurities have not yet been included in the kinetic model.

Kinetic data for the iodine reactions were obtained from the literature, but no data were found for reactions above 60°C. The rate constants for higher temperatures were extrapolated by using an Arrhenius expression which was based on limited temperature-dependent rate and thermodynamic data presented in the earlier report.[1]

2. THE CHEMICAL MODEL

The dynamic behavior of iodine in aqueous media under chemical conditions likely to be encountered in LWR accidents is adequately described by the following set of equations:

$$I_2 + H_2O \underset{k_{-1}}{\overset{k_1}{\rightleftharpoons}} HOI + I^- + H^+ , \quad (1)$$

$$3HOI \underset{k_{-2}}{\overset{k_{20},k_{21}}{\rightleftharpoons}} IO_3^- + 2I^- + 3H^+ , \quad (2)$$

$$4I^- + O_2 + 4H^+ \xrightarrow{k_3} 2I_2 + 2H_2O , \quad (3)$$

$$I_2 + I^- \underset{k_{-4}}{\overset{k_4}{\rightleftharpoons}} I_3^- , \quad (4)$$

$$HOI \overset{K_5}{\rightleftharpoons} H^+ + OI^- , \quad (5)$$

$$H_2O \overset{K_6}{\rightleftharpoons} H^+ + OH^- . \quad (6)$$

The effects of radiation and contaminants are not included in this model. Only the reactions related to hydrolysis and to atmospheric oxygen are included.

Eigen and Kustin[2] measured the rate of relaxation of the rapid equilibration of reaction (1) using the temperature-jump method and obtained a value for k_{-1} at 20°C and an ionic strength of 0.1. They assigned a third-order dependence to this "reverse" reaction step, then calculated the rate constant for the "forward" reaction from the expression

$$k_1 = K_1 k_{-1} , \quad (7)$$

where K_1 is the equilibrium constant for Eq. (1). That study represents the only experimental kinetic data available for Eq. (1) at the present time; hence these results have been used exclusively in our kinetic model. However, the assignment of a third-order rate constant to k_{-1} remains open to criticism, and preliminary experiments at the Oak Ridge National Laboratory (ORNL) indicate that the reaction may be considerably faster than reported by Eigen and Kustin.[2] Furthermore, because this reaction is so rapid (i.e., complete within <1 s), no attempt has been made here to estimate the likely temperature dependence of k_1 or k_{-1}. The kinetics of the analogous reaction of I_3^-, which is a combination of reactions (1)and (4),

$$I_3^- + H_2O \underset{k_{-8}}{\overset{k_8}{\rightleftharpoons}} HOI + 2I^- + H^+ , \quad (8)$$

are unknown. Thus, in the presence of relatively high concentrations of iodine and added iodide, where the I_3^- species may dominate initially, the distribution of all the iodine species as predicted by the model during the initial few seconds of reaction time may also be questioned.

Although HOI is thermodynamically unstable with respect to reduction to I_2 and O_2 in water, the kinetics of this reaction are apparently very slow and undocumented. Therefore, this reaction was not included in the current model.

All of the rate laws proposed previously to describe the formation of iodate shown in Eq. (2) involve second-order rate constants. The most recent study[3] favors a two-term rate law of the form

$$\frac{-d[HOI]}{dt} = k_{20}[HOI]^2 + k_{21}[HOI][OI^-] \quad . \qquad (9)$$

The kinetic measurements supporting the assignment of Eq. (9) are sparse. Only five complete experiments were carried out; however, they encompassed the most crucial pH range of 6 to 10. Moreover, the authors were able to fit the earlier results of Li and White,[4] who conducted more exhaustive meaurements at pH levels of 13 and 14. Therefore, the rate law presented in Eq. (9) has been used, for the most part, in the present model. Nevertheless, the previous rate law proposed by Li and White,[4]

$$\text{Rate of iodate formation} = k'_{20}[OI^-]^2 + k'_{21}[OI^-]^2[I^-]/[OH^-] \quad , \qquad (10)$$

cannot be completely discounted at this time. It has been used in the model on a number of occasions for comparison purposes.[5]

Because of the lack of experimental information on the temperature dependence of either k_{20} or k_{21}, an activation energy of 107 kJ mol^{-1} (25.5 kcal mol^{-1}) for this reaction was estimated from the known activation energy of the reverse reaction[6] and the overall free energy change for reaction (2) was calculated from the energies of formation of the individual species.

The rate of the redox reaction between iodate and iodide represented by the reverse reaction in Eq. (2) was most recently shown[7] to involve a fifth-order rate constant, k_{-2}, in acidic solution. This assignment has been confirmed from experiments conducted at ORNL.[6] Therefore, the following rate law may be written:

$$\text{Rate of disappearance of iodate} = k_{-2}[IO_3^-][I^-]^2[H^+]^2 \quad . \qquad (11)$$

The rate constant (k_3) for the oxidation of iodide, Eq. (3), was determined by Sigalla and Herbo,[8] who established the following rate law for this process:

$$\text{Rate of iodide oxidation} = k_3[I^-][O_2][H^+] \ . \qquad (12)$$

The concentration of oxygen in solution was calculated by assuming that the solution was thoroughly mixed and in equilibrium with the atmosphere, and that Henry's law was obeyed under these conditions. No attempt was made to estimate the temperature dependence of this reaction.

The rate of reaction of I_2 with I^- as shown in Eq. (4) is very rapid and likely to be controlled by diffusion. Temperature-jump experiments have indicated that this reaction is certainly complete within the dead time of the instrument (~2 μs). Therefore, the lower limit for the half-life of reaction (4) was set at 0.2 μs, corresponding to a k_4 value of 3×10^6 M^{-1} s^{-1}. The maximum value of k_4 was suggested[2] to be $<10^{10}$ M^{-1} s^{-1} for a diffusion-controlled reaction. The value of k_{-4} was calculated from the equation

$$k_{-4} = k_4/K_4 \ , \qquad (13)$$

where K_4 is the equilibrium constant for Eq. (4).

$$K_4 = \frac{[I_3^-]}{[I_2][I^-]} \ . \qquad (14)$$

The equilibrium constants for Eqs. (4),[9-14] (5),[15] and (6)[16] are included in the model as the temperature-dependent expressions

$$\ln K_4 = 3727.86/T - 11.6326 + 0.0192212\ T \ , \qquad (15)$$

$$\log K_5 = 2800.48 + 0.7335\ T - 80670./T - 1115.1\ (\log T) \ , \qquad (16)$$

$$\log K_6 = -4.098 - 3245.2/T + 2.2362 \times 10^5/T^2 - 3.984 \times 10^7/T^3 + (13.957 - 1262.3/T + 8.5641 \times 10^5/T^2) \log D_W \ , \qquad (17)$$

where D_W represents the density of water at the saturation vapor pressure of water[17] given by

$$D_W = 1.00017 - 2.36582 \times 10^{-5}\ t - 4.77122 \times 10^{-6}\ t^2 + 8.27411 \times 10^{-9}\ t^3 \ , \qquad (18)$$

and where T and t represent the temperature in K and °C, respectively.

$$T = t + 273.15 \ . \qquad (19)$$

The temperature dependence of K_5, the equilibrium constant for the dissociation of HOI, has not been experimentally determined. In the absence of this information, it has been assumed that the temperature dependence of K_5 follows that for the dissociation of HOBr.[18]

Values of the pertinent rate and equilibrium constants at ambient conditions as used in our kinetic model are shown in Table 1.

In view of the foregoing discussion, we have chosen to model the kinetics of iodine hydrolysis using the following set of differential equations:

$$d[I_2]/dt = -k_1[I_2] + k_{-1}[I^-][HOI][H^+] + 0.5\, k_{p3}[H^+][I^-] - k_4[I_2][I^-] , \tag{20}$$

$$d[I^-]/dt = k_1[I_2] - k_{-1}[I^-][HOI][H^+] + (2/3)k_{20}[HOI]^2 + (2/3)k_{21}[HOI][OI^-] - 2k_{-2}[IO_3^-][I^-]^2[H^+]^2 - k_{p3}[H^+][I^-] - k_4[I_2][I^-] , \tag{21}$$

$$d[HOI]/dt = k_1[I_2] - k_{-1}[I^-][HOI][H^+] - k_{20}[HOI]^2 - k_{21}[HOI][OI^-] + 3k_{-2}[IO_3^-][I^-]^2[H^+]^2 , \tag{22}$$

$$d[IO_3^-]/dt = (1/3)k_{20}[HOI]^2 + (1/3)k_{21}[HOI][OI^-] - k_{-2}[IO_3^-][I^-]^2[H^+]^2 , \tag{23}$$

$$d[I_3^-]/dt = k_4[I_2][I^-] - k_{-4}[I_3^-] + k_{p3}[H^+][I^-] . \tag{24}$$

These equations do not necessarily correspond to the stoichiometry of the chemical equations (1)-(6) because they were derived from experimental observations of the rates of change of the concentrations of individual species involved.

The term $k_{p3}[H^+][I^-]$, which occurs on the right-hand side of Eqs. (20), (21), and (24), accounts for the oxidation of I^- in solution by dissolved oxygen. The complete term would be $k_3[H^+][O_2][I^-]$, where the rate constant k_3 has a value of 3.475×10^{-4} $\underline{M}^{-2}$ s^{-1}, as reported by Sigalla and Herbo.[8] If we assume that Henry's law is obeyed by the dissolved oxygen and that the solution is in equilibrium with the oxygen of the atmosphere at all times, then the concentration of oxygen in solution remains at 2.69×10^{-4} $\underline{M}$. Hence $k_3[O_2]$ may be replaced by k_{p3} with a value of 9.35×10^{-8} $\underline{M}^{-1}$ s^{-1}.

Note that under the original experimental conditions used to determine k_3 the iodide concentration was sufficiently high to ensure that all the iodine generated was immediately converted to I_3^-. Although I_3^- is not a major constituent under the conditions bracketed by our calculations, the last term in Eq. (24) is included to preserve the overall validity of the model.

Table 1. Values of rate and equilibrium constants used in the kinetic model at ambient conditions

Constant	Temperature °C	Value	Reference
k_1[a]	20	$3\ s^{-1}$	2
k_{-1}	20	$4.4 \times 10^{12}\ \underline{M}^{-2}\ s^{-1}$	2
k_{20}	25	$250\ \underline{M}^{-1}\ s^{-1}$	3
k_{21}	25	$120\ \underline{M}^{-1}\ s^{-1}$	3
k_{-2}	25	$3 \times 10^{8}\ \underline{M}^{-4}\ s^{-1}$	7
k_3	25	$3.475 \times 10^{-4}\ \underline{M}^{-2}\ s^{-1}$	8
k_4	25	$3 \times 10^{6}\ \underline{M}^{-1}\ s^{-1}$	Estimated[b]
k_{-4}	25	$4 \times 10^{3}\ s^{-1}$	Estimated[b]
K_4	25	736	9-15
K_5	25	2.3×10^{-11}	16
K_6	25	1.006×10^{-14}	17

[a]The value of k_1 was calculated by Eigen and Kustin,[2] who assumed that $K_1 = 6.8 \times 10^{-13}\ \underline{M}^2$.

[b]At press time, the authors found experimental values for k_4 and k_{-4}. These rate constants were reported [D. H. Turner, G. W. Flynn, N. Sutin, and J. V. Beitz, J. Am. Chem. Soc. 94, 1554 (1972)] to be $6.2 \times 10^{9}\ \underline{M}^{-1}\ s^{-1}$ and $8.5 \times 10^{6}\ s^{-1}$ at 25°C, respectively, both of which are three orders of magnitude greater than the estimated values used in the calculations. The use of the experimental values will not significantly change the calculated results presented in this report.

The set of differential equations [Eqs. (20) through (24)] representing the rates of formation and disappearance of the various species encountered in the hydrolysis of iodine was solved numerically using computer program IRATE (see Appendix) to yield the concentrations of each species as a function of time. The calculations were performed over the pH range 4 to 11 at 25°C with initial I_2 concentrations of 10^{-3} to 10^{-7} and 10^{-9} M; and at pH levels of 5, 7, and 9 at 60, 100, and 125°C with initial I_2 concentrations of 10^{-4}, 10^{-5}, 10^{-7}, and 10^{-9} M. The results are presented in Figs. 1-29 in Sect. 5.

The first method used in solving the differential equations involved a variable-step, fourth-order Runge-Kutta integration scheme.[19] With this method we were able, under some conditions, to calculate the concentrations of the various hydrolytic species of iodine as a function of time over periods extending to several months without using an exorbitant amount of computing time (e.g., no more than a few minutes per run). However, in some cases, especially at the lower pH values and the lower temperatures, the calculations became very time-consuming, requiring as much as 15 min of computer time to extend the calculations out to 100 s. Such behavior, which is encountered when one solves differential equations using a forward difference scheme such as Runge-Kutta, may be attributed to the property of "stiffness" inherent in the set of differential equations under a certain range of conditions. In kinetic calculations, stiffness may arise when some variables change on time scales very different from others. This is the case with iodine hydrolysis. When stiffness is encountered, a method such as Runge-Kutta, which is satisfactory for "nonstiff" problems, becomes inefficient (as in our experience).

After encountering the problem of stiffness in solving our set of differential equations, we adopted a modified Gear method[20] based on a backward difference scheme which uses a Jacobian matrix for solving the set of nonlinear equations obtained in the expansion of the differential equations. This method proved to be very efficient for solving our set of differential equations under any conditions of temperature, pH, and total concentration of iodine. Hence we used it (see computer program IRATE in Appendix) to extend all the calculations to ~30 years, with a time expenditure of only a few seconds of computer time per run.

3. PARTITION COEFFICIENTS

The previous report[1] presented partition coefficients between the aqueous and gaseous phases for iodine systems at equilibrium without the influence of radiation or contamination. It was shown that in aqueous systems simulating LWR accident conditions of temperature, concentration, pH, and large volumes of water, an iodine source as I_2 would react and form nonvolatile species. Also considered was a "hypothetical" iodine solution in which only the hydrolysis reaction took place (i.e., no

iodate was formed). The calculated pseudoequilibrium partition coefficients obtained for this case were labeled as the lowest possible iodine partition coefficients. Thus, a nonequilibrium solution of iodine will exhibit partition coefficients between those of the two above extremes.

The partition coefficient for an individual iodine species is defined as the ratio of the concentration of that species in the liquid phase to its concentration in the vapor phase. The volatility of this species, then, is the reciprocal of this coefficient. Likewise, the overall partition coefficient for an aqueous iodine system is represented by the ratio of the sum of the aqueous-phase concentrations to the gas-phase concentrations. Then, for a system free of organic materials and with HOI and I_2 as volatile species, the iodine partition coefficient, PC, is

$$\frac{\Sigma[I]_a}{\Sigma[I]_g} = \frac{[I^-]_a + [IO_3^-]_a + [I_3^-]_a + [HOI]_a + [I_2]_a + [OI^-]_a}{[HOI]_g + [I_2]_g} , \qquad (25)$$

and it is obvious that the reciprocals of these partition coefficients would be aqueous iodine volatility coefficients.

The overall partition coefficients were calculated from the individual partition coefficients for HOI and I_2 and from the concentrations of all the iodine species in the aqueous phase. The equilibrium between the phases was assumed to be instantaneous; furthermore, the amount of iodine transferred between phases was presumed to be insignificant compared with the total. Eggleton[21] concluded that good partition coefficients for I_2 were 83 and 9.1 for 25 and 100°C, respectively, and that the coefficient for HOI at 25°C should be several thousand. However, Kabat[22] suggested that a more conservative value of a few hundred should be used for HOI. We have selected three values, 400, 1000, and 5000, for estimates of the partition coefficient of HOI at 25°C and have taken the corresponding estimates of coefficients for HOI at 100°C to be 40, 100, and 500, or values that are lower by about the same factor as those for I_2. The previous report[1] included aqueous iodine equilibrium partition coefficients with the HOI partition coefficient conservatively assumed to be a factor of 2 greater than that for I_2 (i.e., 186 and 19.2 at 25 and 100°C, respectively). We now believe that the real HOI partition coefficient at 25°C will be no less than 400 and may be as large as several thousand.

Plots of the calculated partition coefficients vs time are presented in Figs. 30-35 (in Sect. 5) for solutions with total iodine concentrations of 10^{-5}, 10^{-7}, and 10^{-9} M at pH levels of 5, 7, and 9, and temperatures of 25 and 100°C. Each figure shows how total partition coefficients change with time for a given total iodine concentration at the three pH conditions and the two temperatures. At high pH levels (low acid concentrations), reactions (1) and (2) proceed readily toward formation of the ionic products; thus, a high pH decreases the effective iodine volatility and, in turn, increases the partition coefficients.

4. SUMMARY AND CONCLUSIONS

The following conclusions can be drawn from the results obtained in this study:

1. Increasing the pH of an iodine solution (10^{-9} up to 10^{-3} g-atom/L) to 7 or higher markedly increases the reaction rates to form iodide and iodate (Figs. 1–16). Indeed, pH appears to be the most important variable in determining not only the equilibrium speciation of iodine, but also the rate at which equilibrium is attained. Thus, any effort to increase the pH of iodine-contaminated water resulting from a nuclear accident would be rewarded by the stabilization of iodine in the form of the nonvolatile species, iodide and iodate; more importantly, it would ensure an increase in the rate at which this final species distribution is attained.

2. As expected, the rate of disproportionation of iodine increases with increasing temperature (Figs. 17–29). Moreover, as illustrated by the equilibrium model, the concentration of HOI relative to the initial iodine concentration also increases with temperature, as does the concentration of OI^-, although this latter species has only a minor role in the pH range of interest to LWR accident chemistry. However, the kinetic model demonstrates that HOI is more short-lived at higher temperatures and represents less of a potential threat to the environment for much shorter times under these conditions.

As a by-product of this investigation, one can now establish the experimental conditions and the time frame that HOI may be an observable species in solution, thereby facilitating its characterization and the measurement of its properties.

3. Decreasing the initial concentration of iodine also tends to slow the overall rate of reaction to form iodate and iodide and to increase the relative importance of HOI in solution. However, the actual amounts of the two volatile species, I_2 and HOI, also decrease. In fact, the total iodine concentration in cases where HOI becomes a relatively major species is so low as to render HOI virtually innocuous. This conclusion leads to another point, namely, that in order to determine partition coefficients for HOI at very low concentrations of initial I_2 ($\leq 10^{-7}$ M) one would have to obtain extremely pure water (which was not already contaminated with equivalent concentrations of iodide). Furthermore, the methods of detection become insensitive at these lower limits. Even the use of radioisotopes of iodine to determine partition coefficients introduces unknown levels of stable iodide.

4. Equation (3) was introduced into the model for the sake of completeness. However, despite the fact that the oxygen concentration was considered to exist at its maximum level (i.e., the solution is in equilibrium with the air at all times and fully saturated with oxygen),

this reaction had no apparent effect on the iodide concentration over the simulated reaction time of ~32 years.

Other important processes that have not yet been incorporated into the model include radiolysis, photolysis, and catalysis (e.g., redox reactions with other impurities in the containment wa :). However, these processes were not considered at this time beca e they are very complex and involve a number of site-specific assumptions.

5. Recent measurements of the rate of disproportionation of I_2 to form HOI and I^-, Eq. (1), indicate that this reaction may be orders of magnitude faster than was previously reported. However, until these results are confirmed, the data of Eigen and Kustin[2] will be used in the current model. Moreover, this reaction is so fast that it can be considered virtually insta taneous in any applicat ion to nuclear accident scenarios. For this reason, no attempt was made in the model to estimate the temperature dependence of this reaction.

6. A number of reactions need to be reinvestigated. Most importantly, the rate law for the formation of iodate and iodide in Eq. (2) must be established unequivocally. It should be noted that the currently accepted rate law of Thomas et al.[3] was obtained from a limited number of experiments at pH values $\geq$7. Although the agreement between the values for the equilibrium concentrations of the major species, iodide and iodate, obtained by the kinetic model and the equilibrium model[1] for the same experimental conditions is quite adequate at pH $\geq$7, it becomes progressively less satisfactory at lower pH values; in particular, the concentrations of iodine predicted by both models vary considerably under these conditions. The equilibrium concentrations of iodide and iodate calculated from the kinetic model are generally larger than those derived from the equilibrium model, while the concentrations of the remaining species are smaller. These differences can be reduced by assuming a smaller value for k_{20} (the k_{20} term in Eq. (9) overwhelms the k_{21} term in the low pH region). It is interesting to note that the value of k_{20} reported by Li and White[4] is only 0.05 $\underline{M}^{-1}$ s^{-1} (cf. 250 $\underline{M}^{-1}$ s^{-1} in Table 1) and gives better agreement between the equilibrium and kinetic models, even though their constant strictly pertains to the OI^- ion and there is no evidence that HOI and OI^- are equally reactive with respect to disproportionation. In any event, the results obtained from the kinetic model using a rate law adapted from that of Li and White[4] (who conducted their experiments in the pH range of 13 to 14) are very compatible with the results presented in this report at pH >9. However, the two sets of data diverge markedly as the pH is decreased below 9.

7. Finally, once the rate law for the production of iodate, Eq. (9), is definitely defined, the temperature and ionic strength dependencies of the resulting rate constants need to be measured.

5. RESULTS OF CALCULATIONS

The results of the calculations made in this study are presented in the form of plots of the concentrations of iodine species as a function of time (Figs. 1-29) and plots of iodine partition coefficients as a function of time (Figs. 30-35). The conditions used in making these calculations are discussed in Sects. 2 and 3.

Figures 1-16 are arranged in consecutive pairs (i.e., Figs. 1 and 2 face each other, Figs. 3. and 4 face each other, etc.) so that the reader is provided with a continuity of concentration range for each pH level.

ORNL DWG 82-308

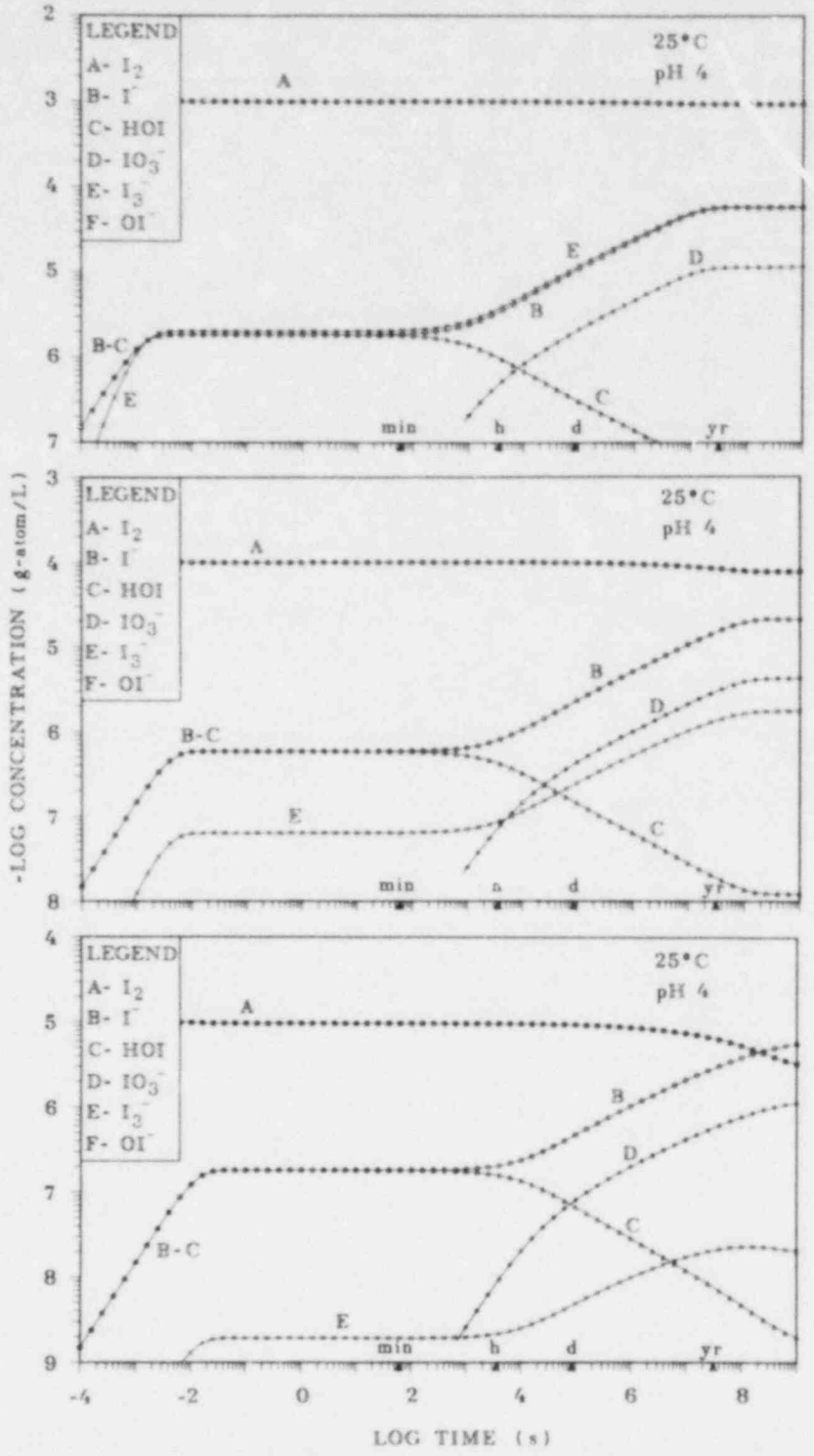

Fig. 1. Concentrations of iodine species as a function of time when 10^{-3}, 10^{-4}, and 10^{-5} g-atom/L of I_2 equilibrates in water at 25°C with a buffered pH of 4.

ORNL DWG 82-453

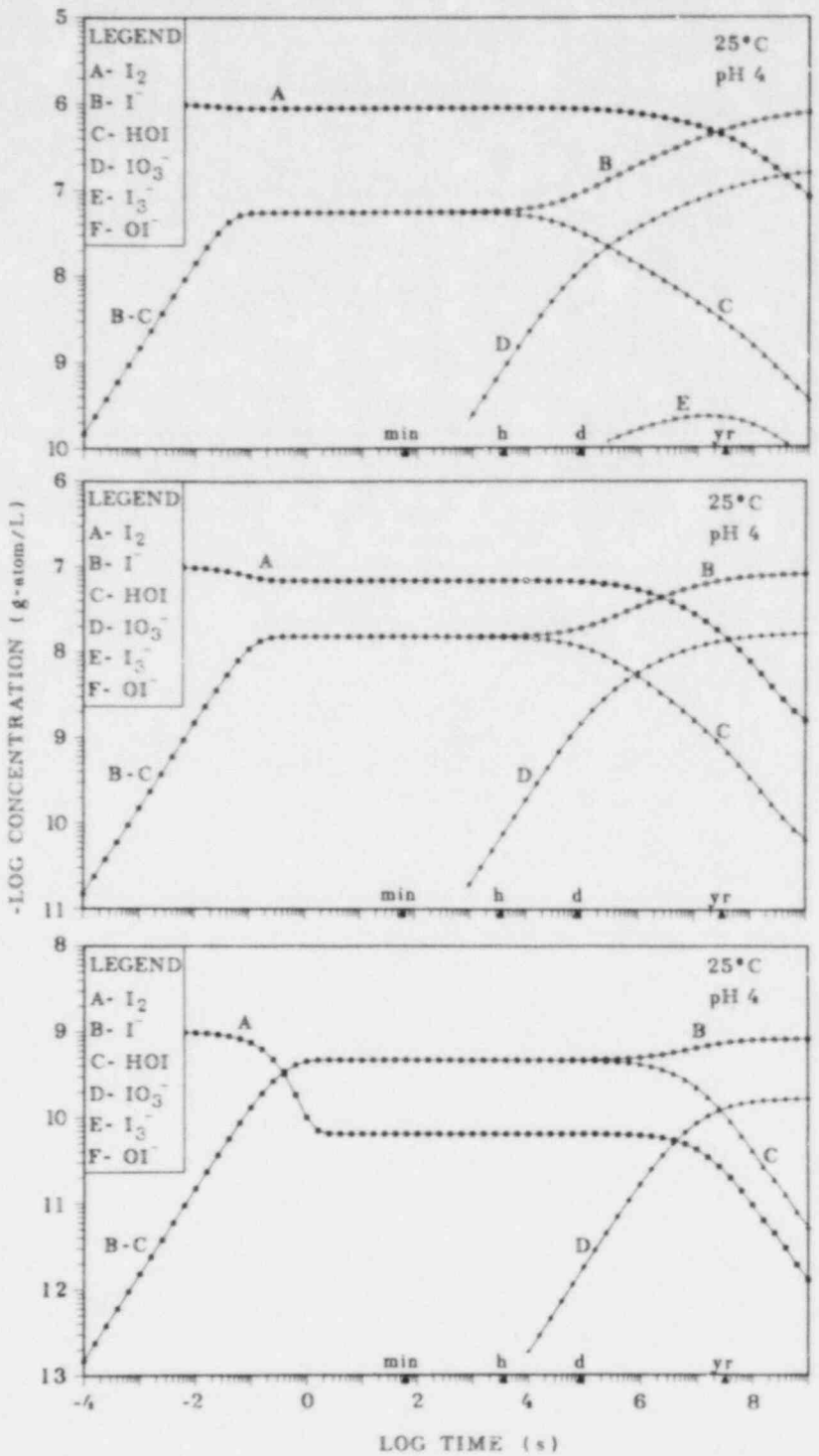

Fig. 2. Concentrations of iodine species as a function of time when 10^{-6}, 10^{-7}, and 10^{-9} g-atom/L of I_2 equilibrates in water at 25°C with a buffered pH of 4.

ORNL DWG 82-266

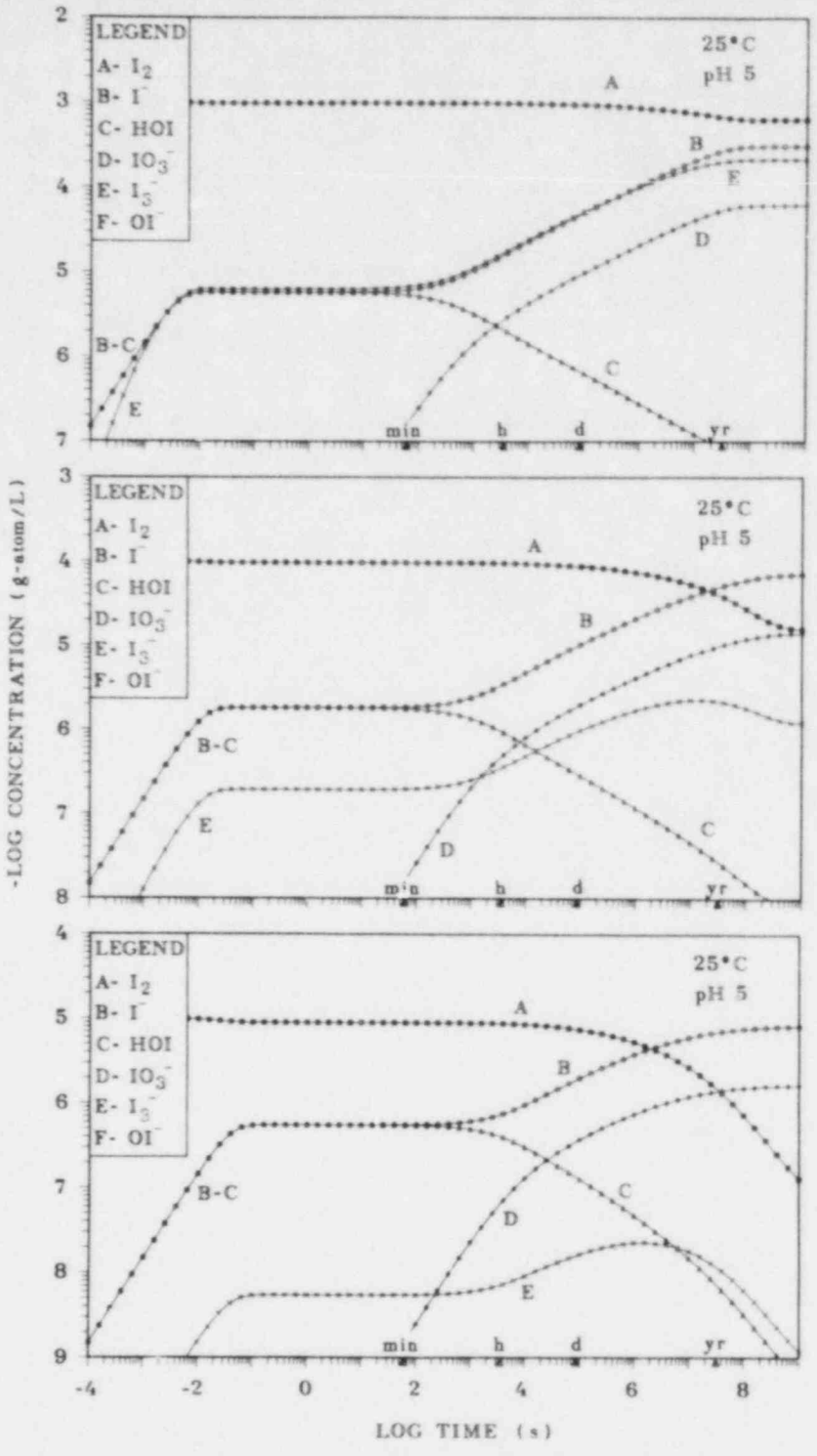

Fig. 3. Concentrations of iodine species as a function of time when 10^{-3}, 10^{-4}, and 10^{-5} g-atom/L of I_2 equilibrates in water at 25°C with a buffered pH of 5.

ORNL DWG 82-454

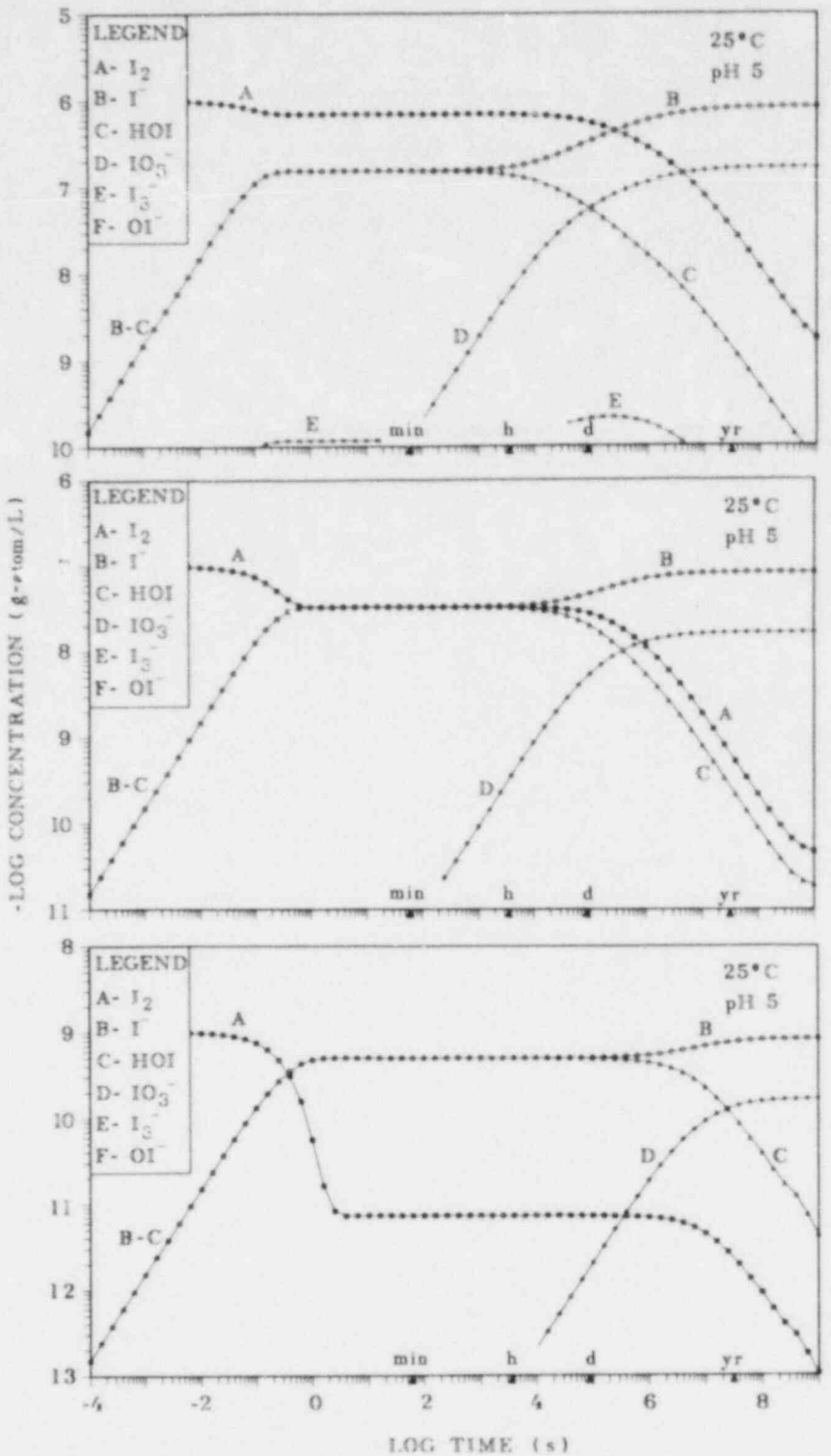

Fig. 4. Concentrations of iodine species as a function of time when 10^{-6}, 10^{-7}, and 10^{-9} g-atom/L of I_2 equilibrates in water at 25°C with a buffered pH of 5.

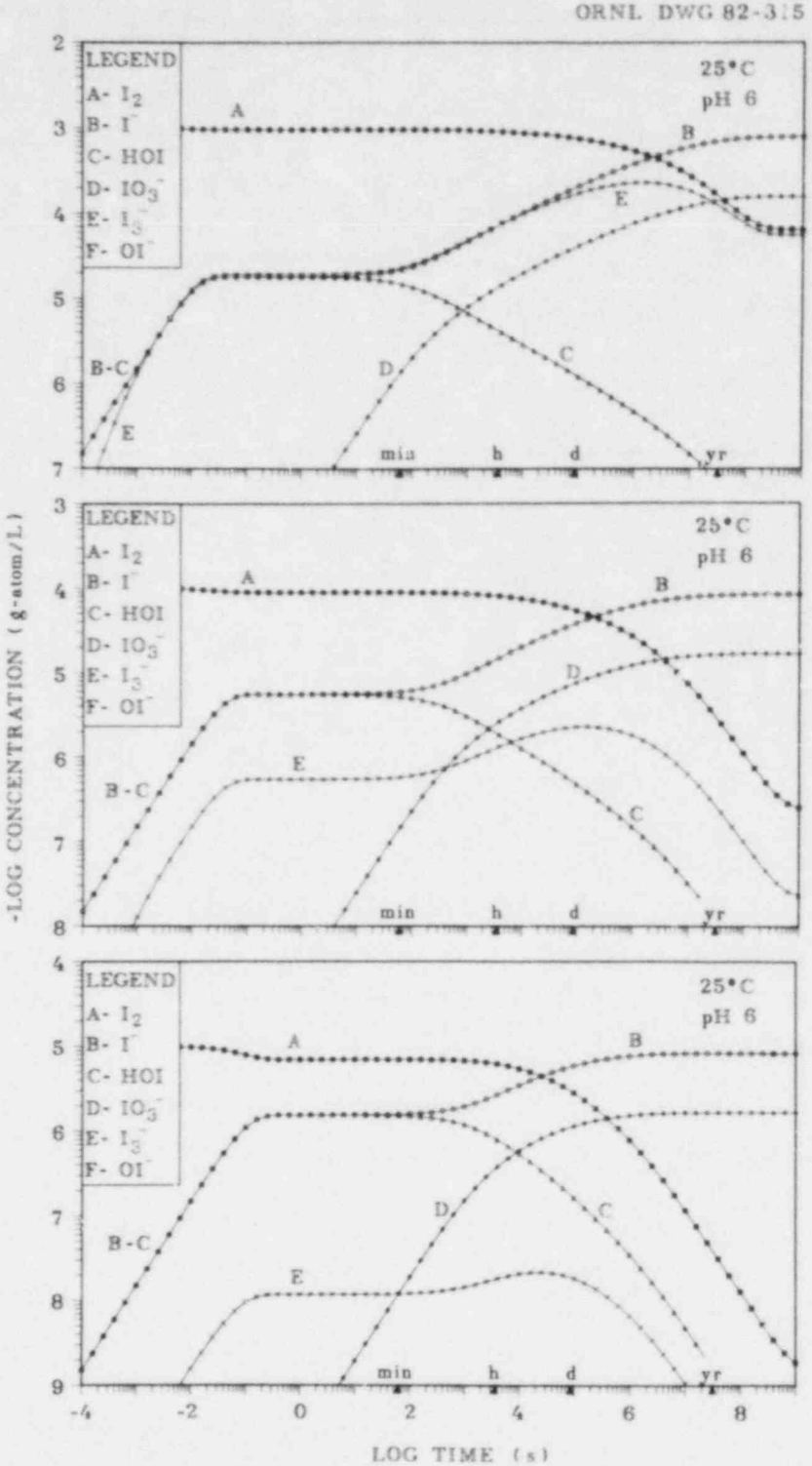

Fig. 5. Concentrations of iodine species as a function of time when 10^{-3}, 10^{-4}, and 10^{-5} g-atom/L of I_2 equilibrates in water at 25°C with a buffered pH of 6.

ORNL DWG 82-307

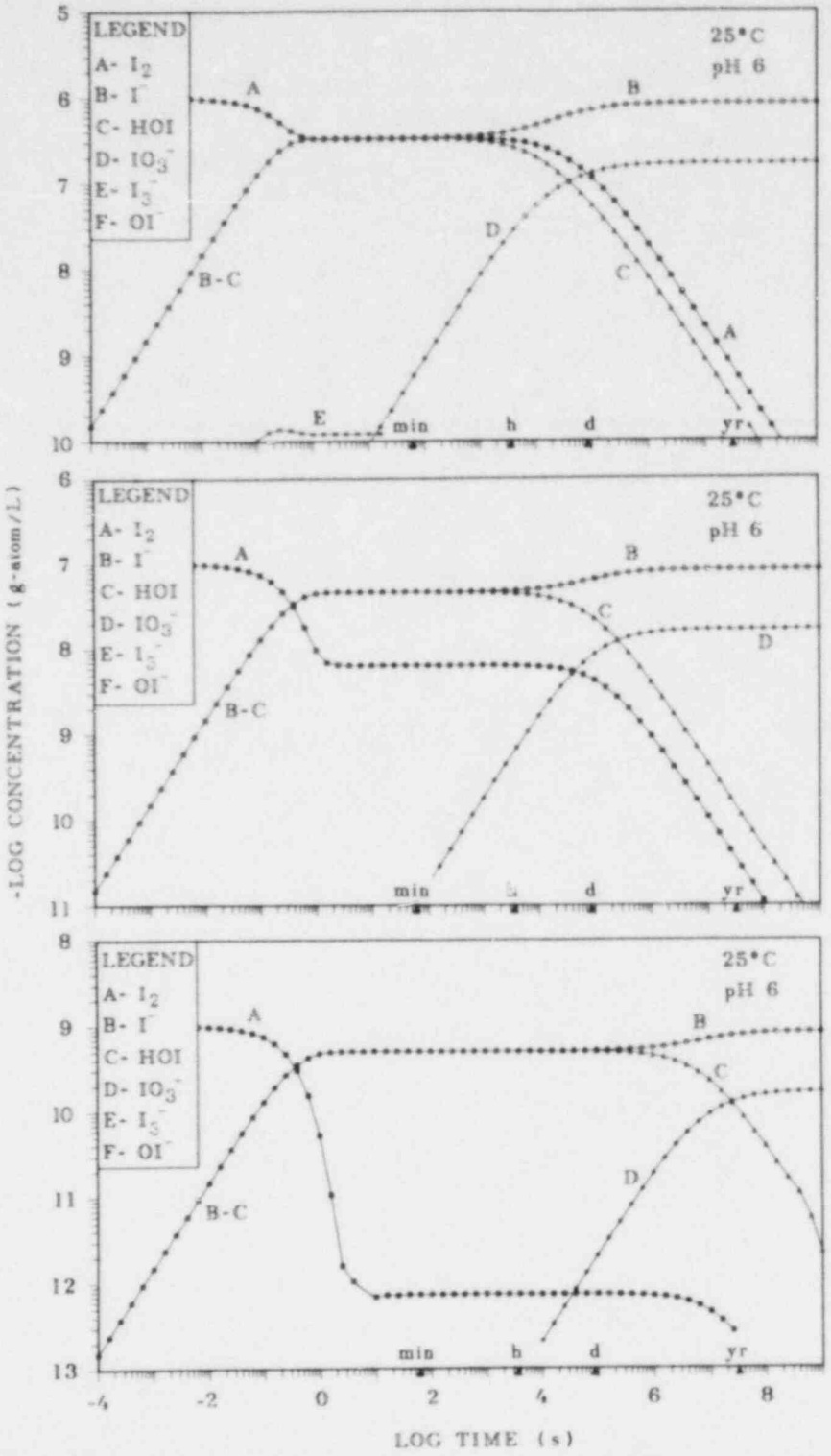

Fig. 6. Concentrations of iodine species as a function of time when 10^{-6}, 10^{-7}, and 10^{-9} g-atom/L of I_2 equilibrates in water at 25°C with a buffered pH of 6.

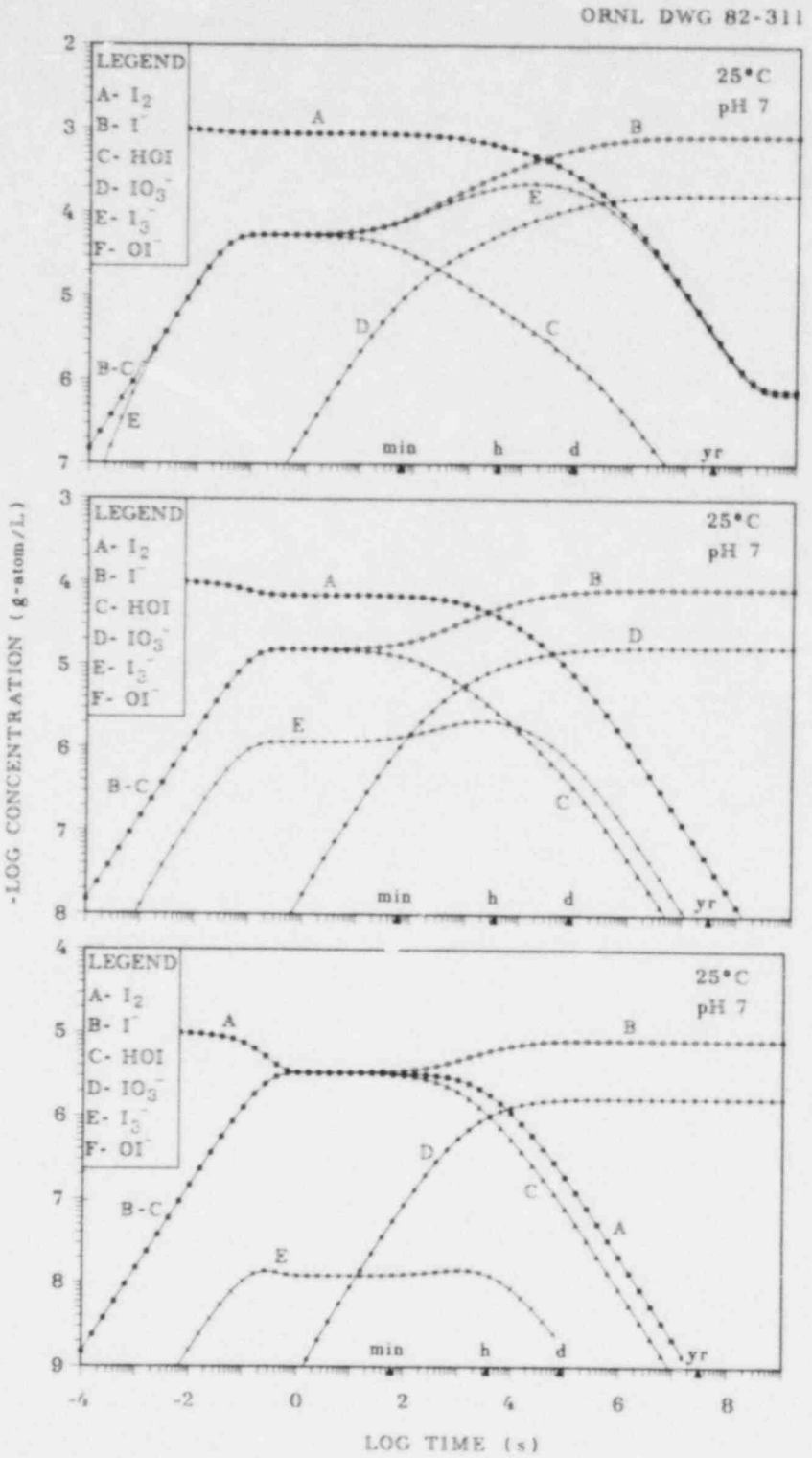

Fig. 7. Concentrations of iodine species as a function of time when 10^{-3}, 10^{-4}, and 10^{-5} g-atom/L of I_2 equilibrates in water at 25°C with a buffered pH of 7.

ORNL DWG 82-449

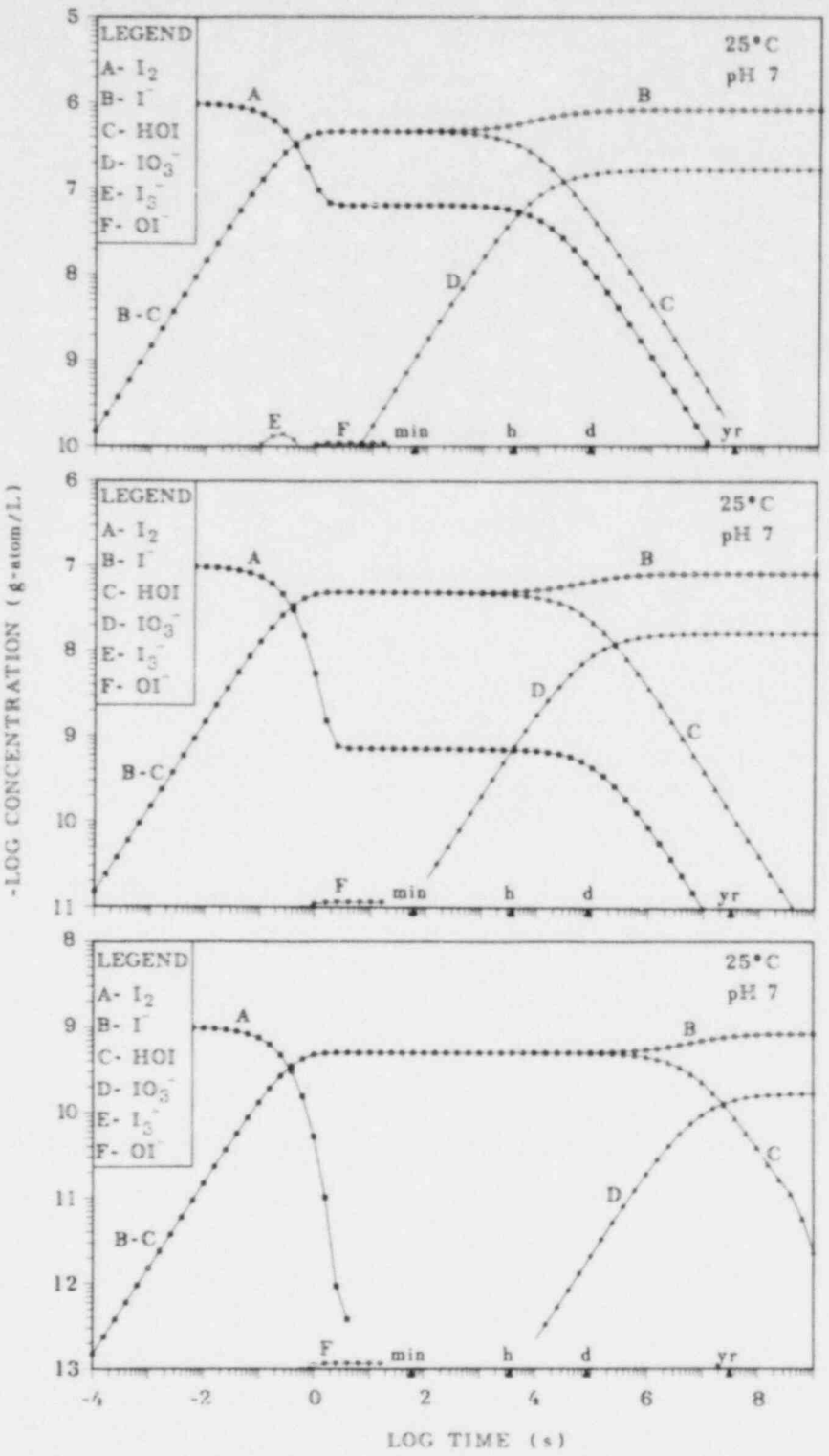

Fig. 8. Concentrations of iodine species as a function of time when 10^{-6}, 10^{-7}, and 10^{-9} g-atom/L of I_2 equilibrates in water at 25°C with a buffered pH of 7.

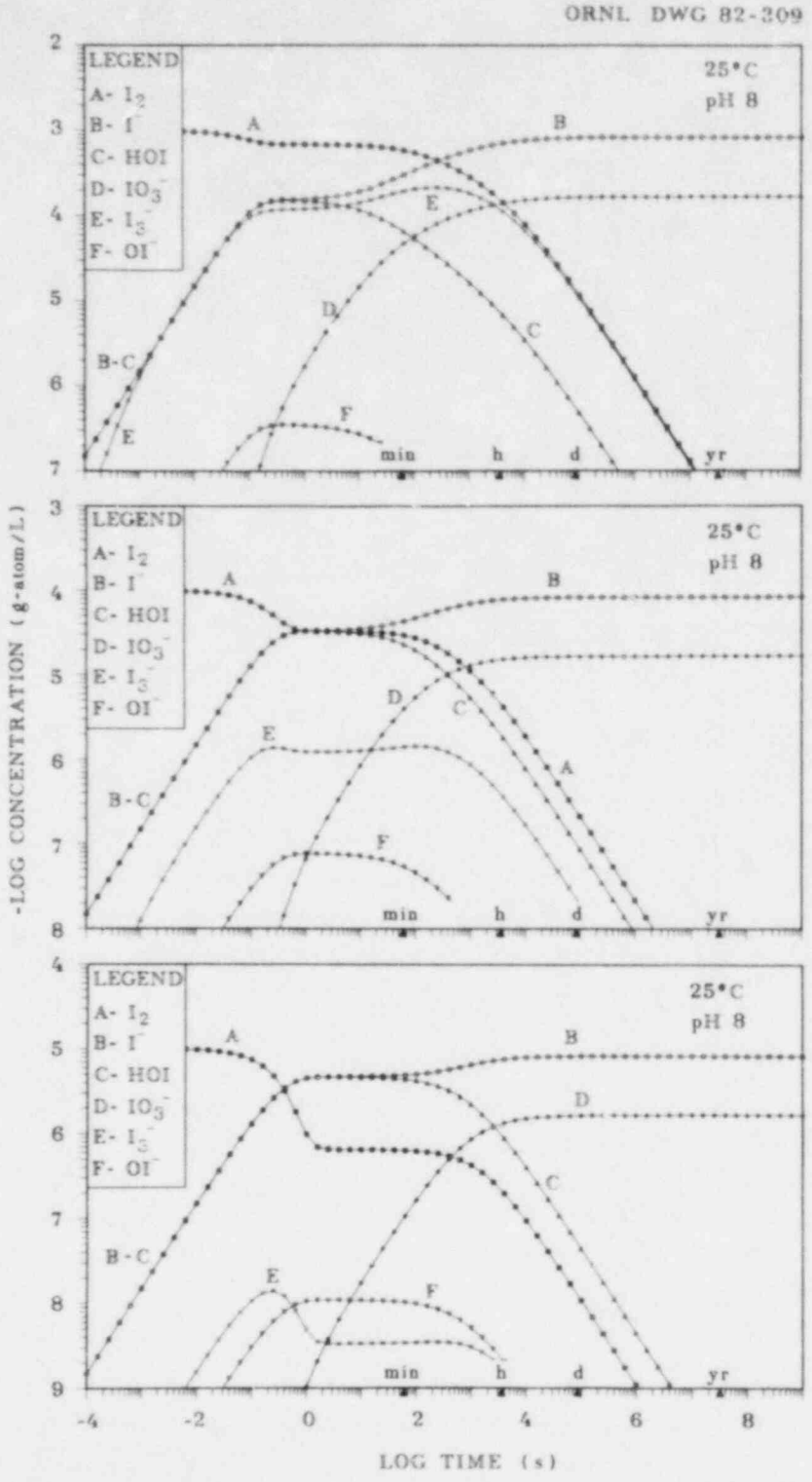

Fig. 9. Concentrations of iodine species as a function of time when 10^{-3}, 10^{-4}, and 10^{-5} g-atom/L of I_2 equilibrates in water at 25°C with a buffered pH of 8.

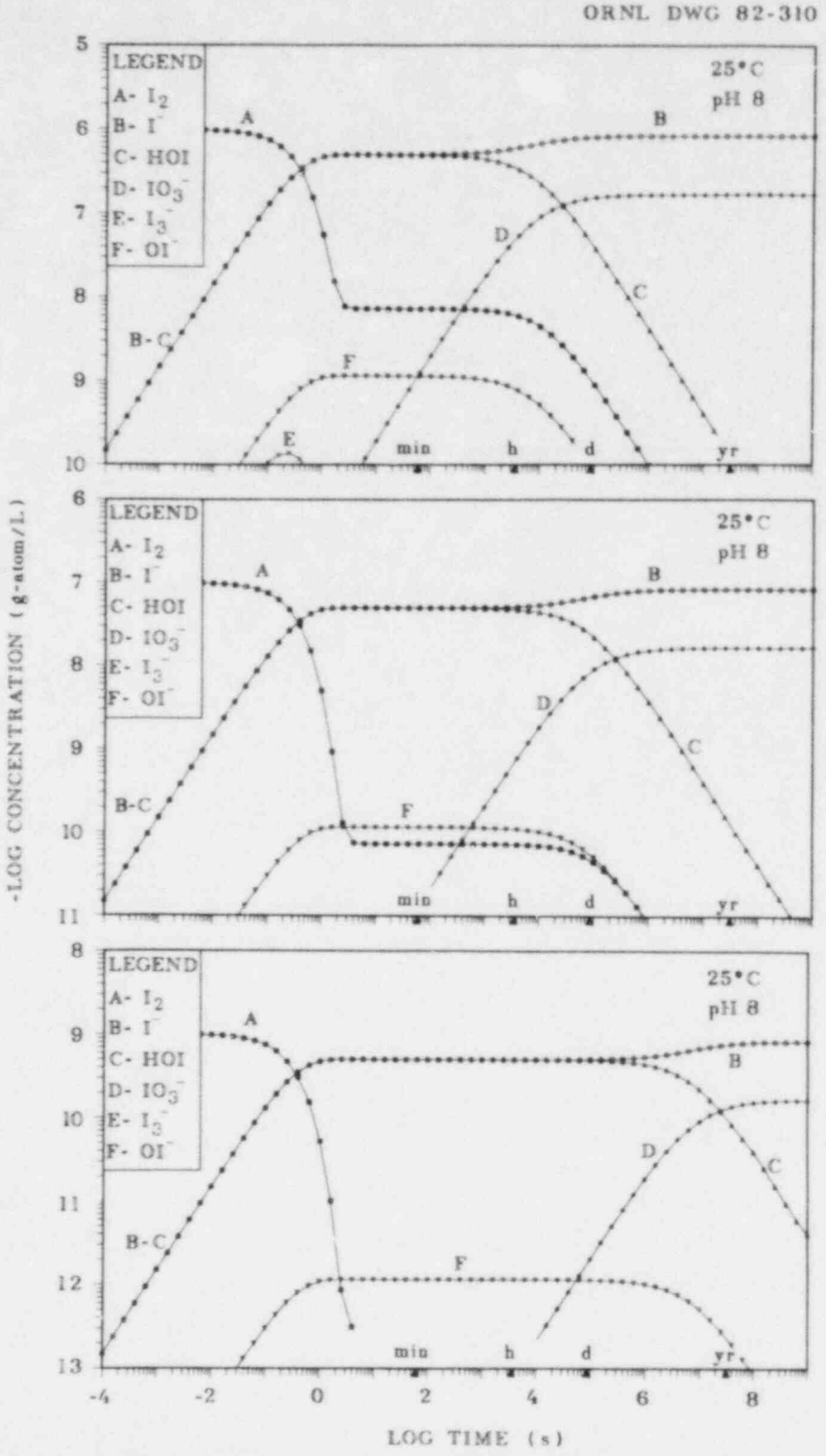

Fig. 10. Concentrations of iodine species as a function of time when 10^{-6}, 10^{-7}, and 10^{-9} g-atom/L of I_2 equilibrates in water at 25°C with a buffered pH of 8.

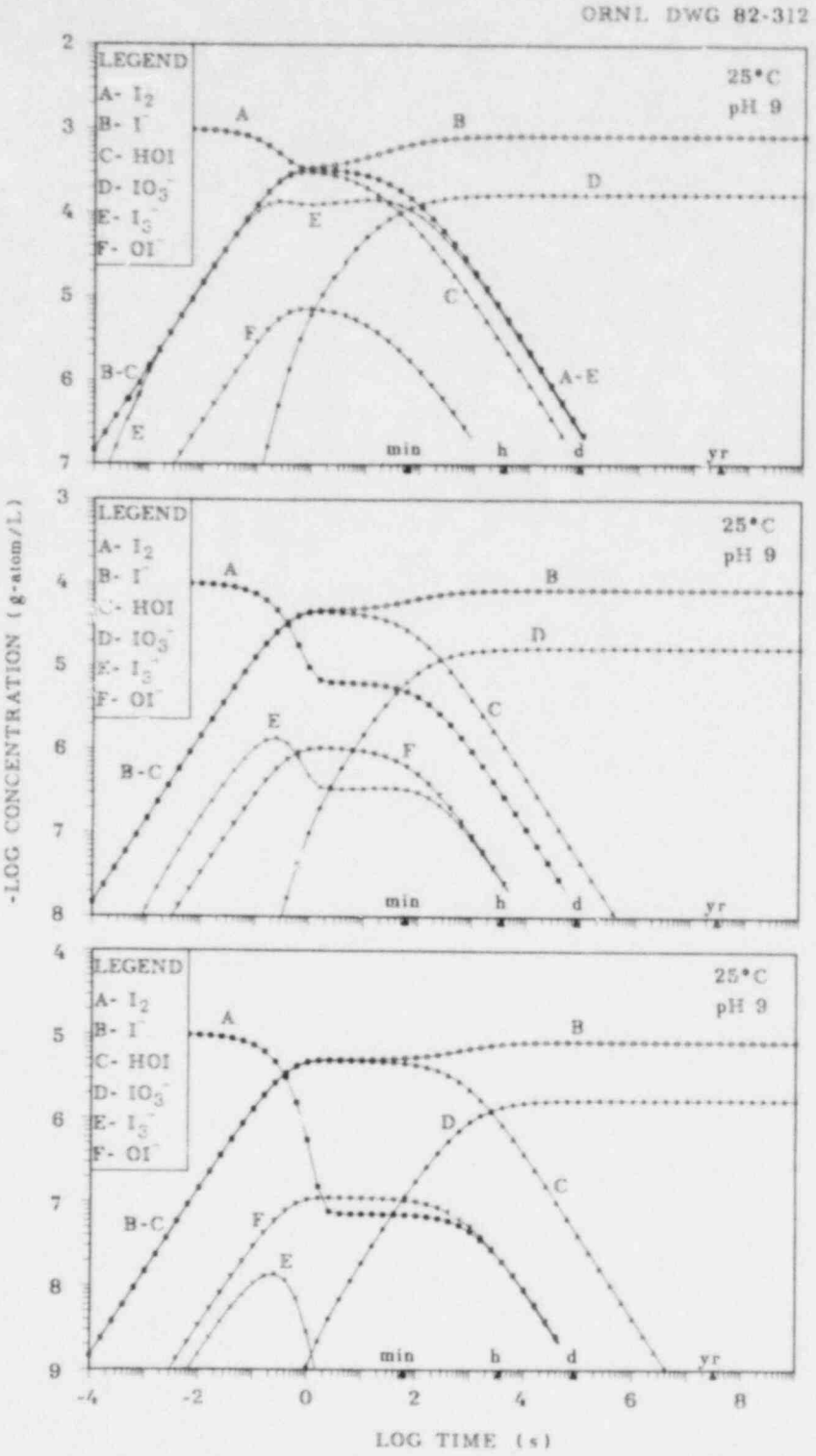

Fig. 11. Concentrations of iodine species as a function of time when 10^{-3}, 10^{-4}, and 10^{-5} g-atom/L of I_2 equilibrates in water at 25°C with a buffered pH of 9.

ORNL DWG 82-451

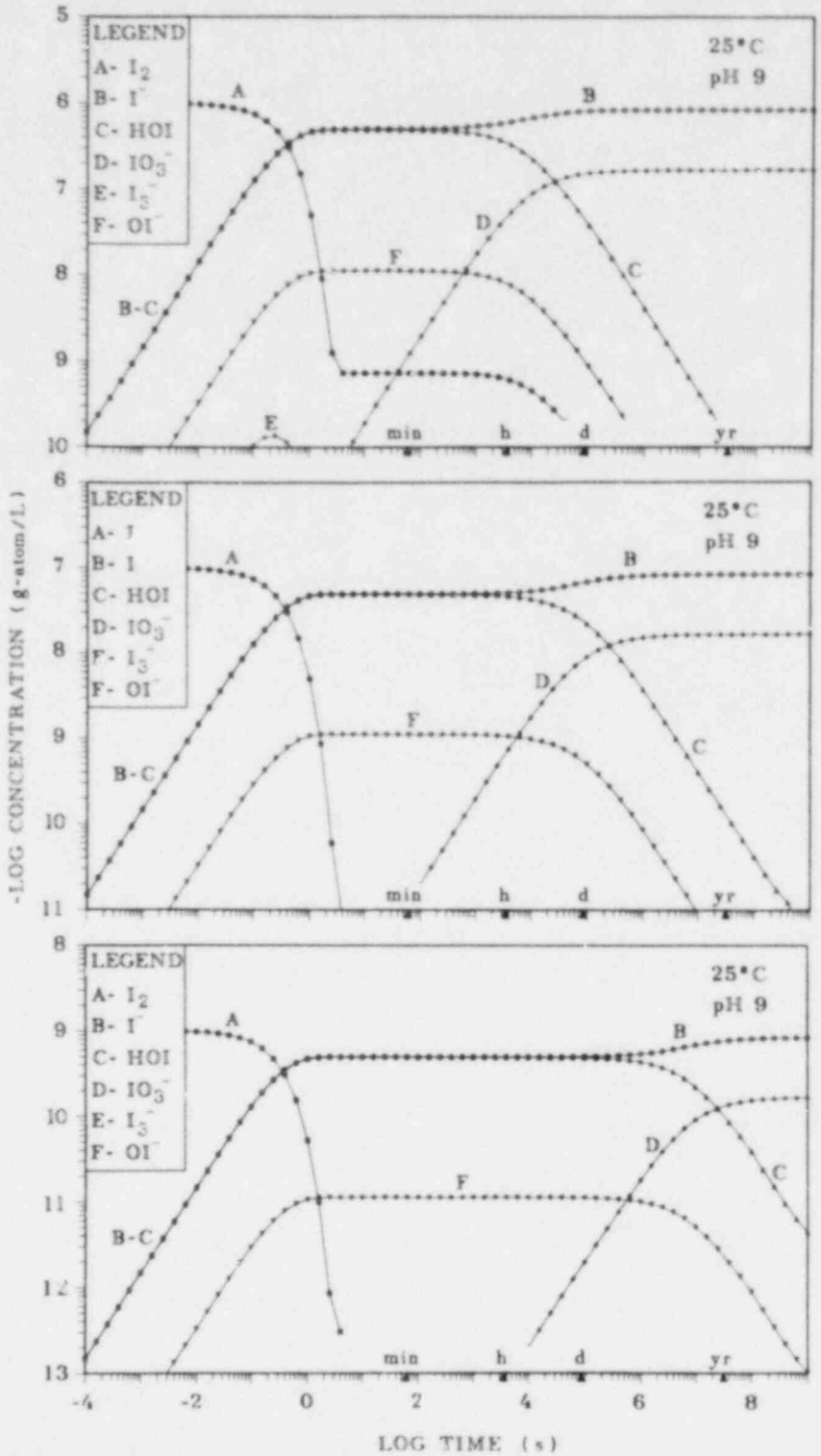

Fig. 12. Concentrations of iodine species as a function of time when 10^{-6}, 10^{-7}, and 10^{-9} g-atom/L of I_2 equilibrates in water at 25°C with a buffered pH of 9.

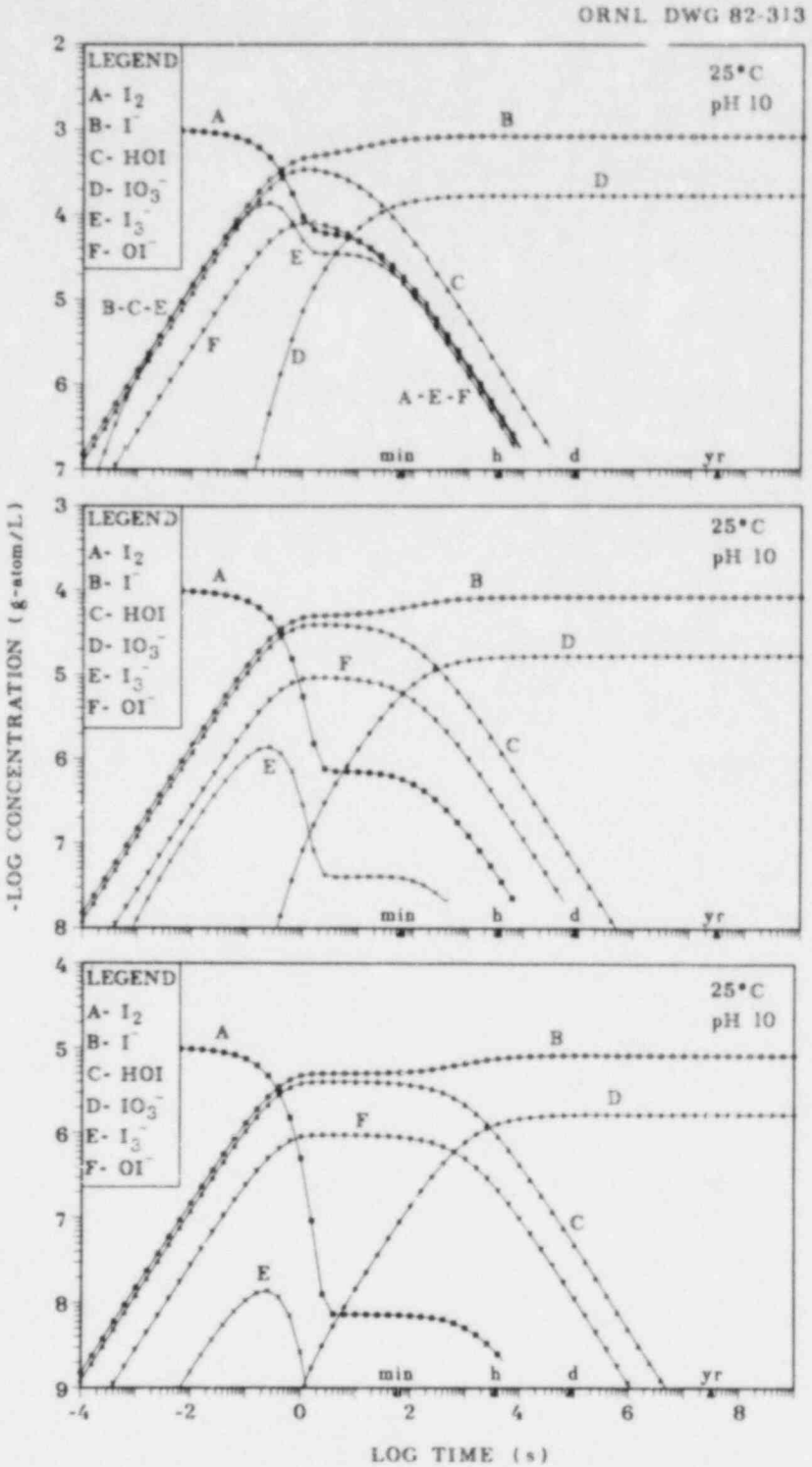

Fig. 13. Concentrations of iodine species as a function of time when 10^{-3}, 10^{-4}, and 10^{-5} g-atom/L of I_2 equilibrates in water at 25°C with a buffered pH of 10.

ORNL DWG 82-452

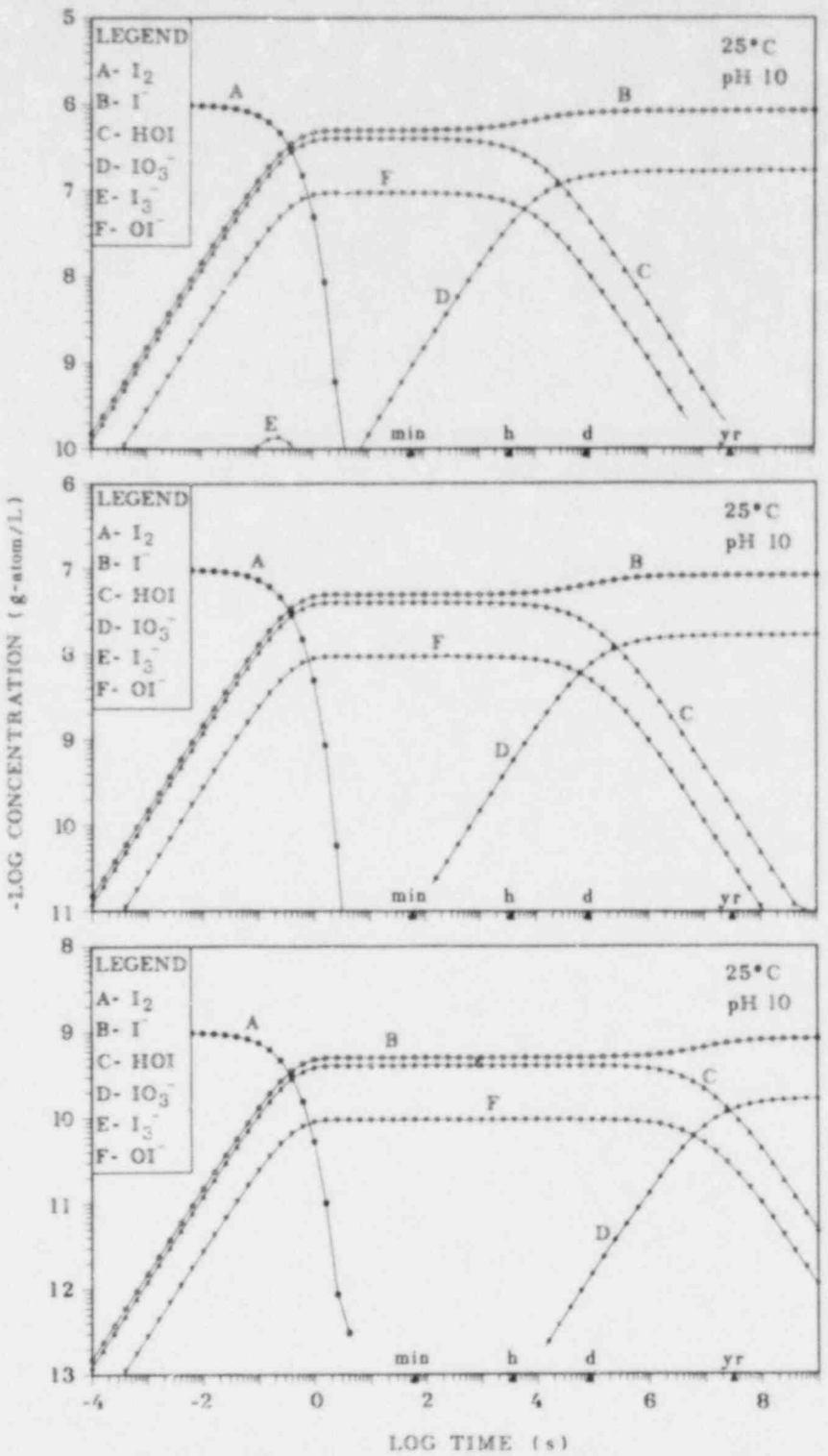

Fig. 14. Concentrations of iodine species as a function of time when 10^{-6}, 10^{-7}, and 10^{-9} g-atom/L of I_2 equilibrates in water at 25°C with a buffered pH of 10.

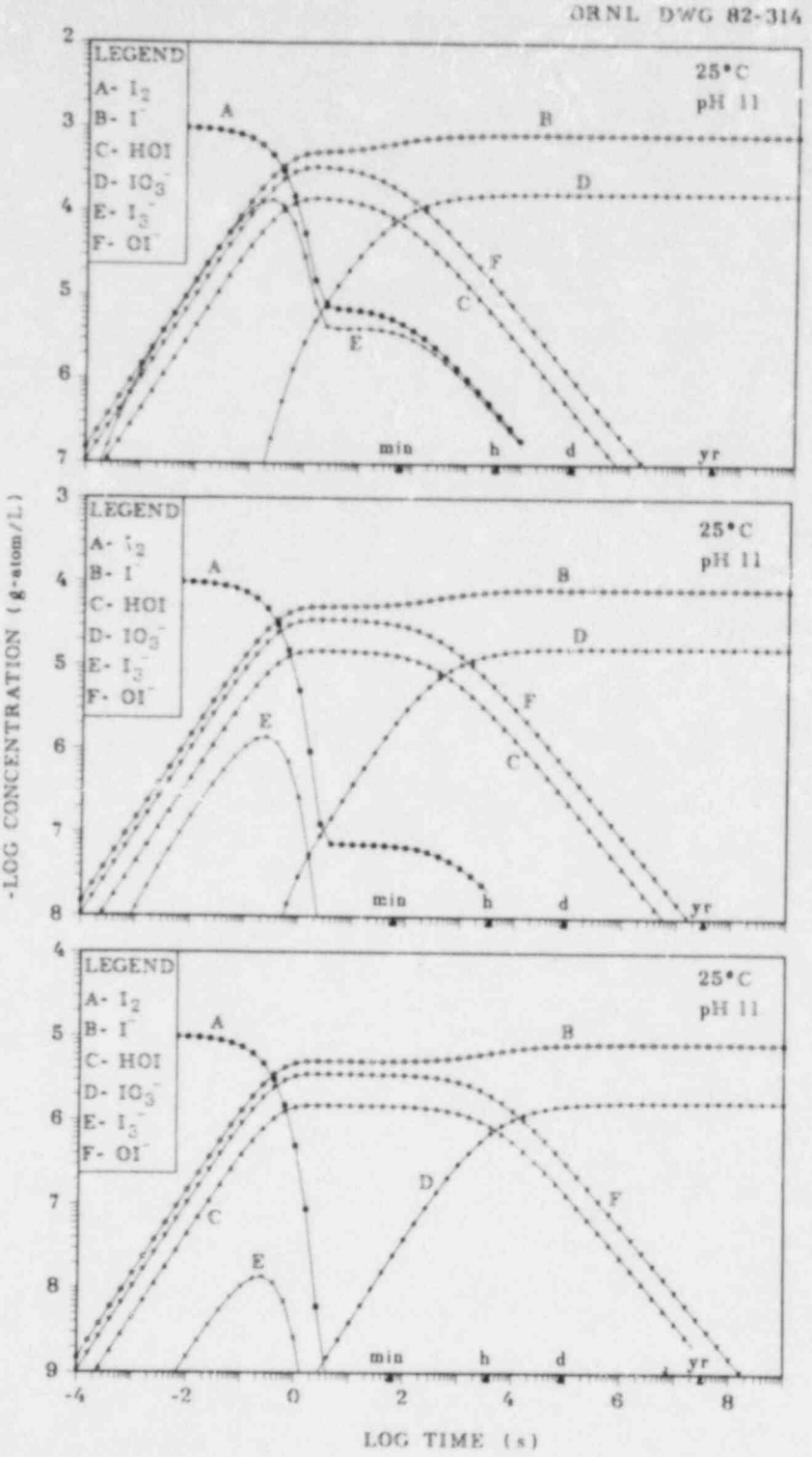

Fig. 15. Concentrations of iodine species as a function of time when 10^{-3}, 10^{-4}, and 10^{-5} g-atom/L of I_2 equilibrates in water at 25°C with a buffered pH of 11.

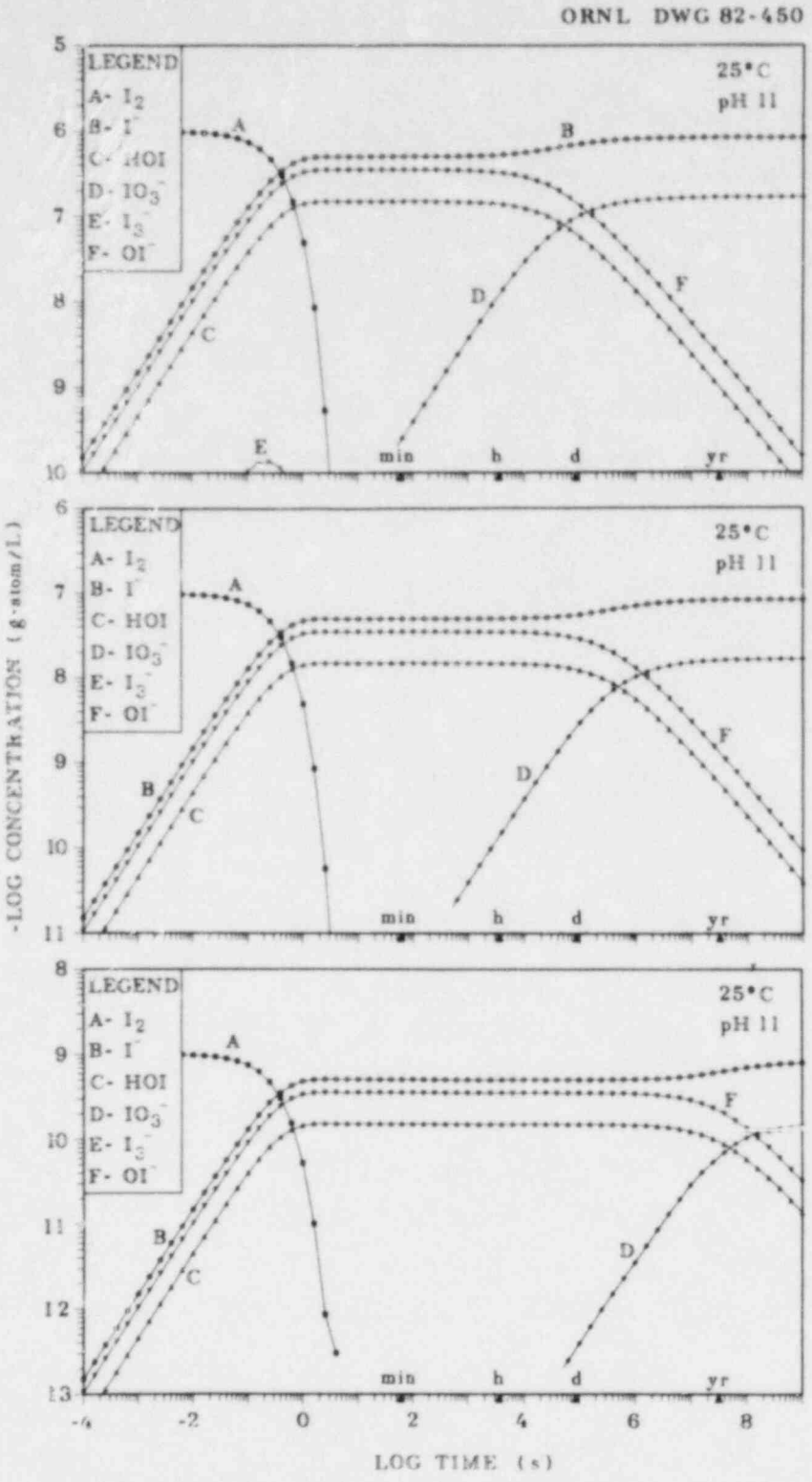

Fig. 16. Concentrations of iodine species as a function of time when 10^{-6}, 10^{-7}, and 10^{-9} g-atom/L of I_2 equilibrates in water at 25°C with a buffered pH of 11.

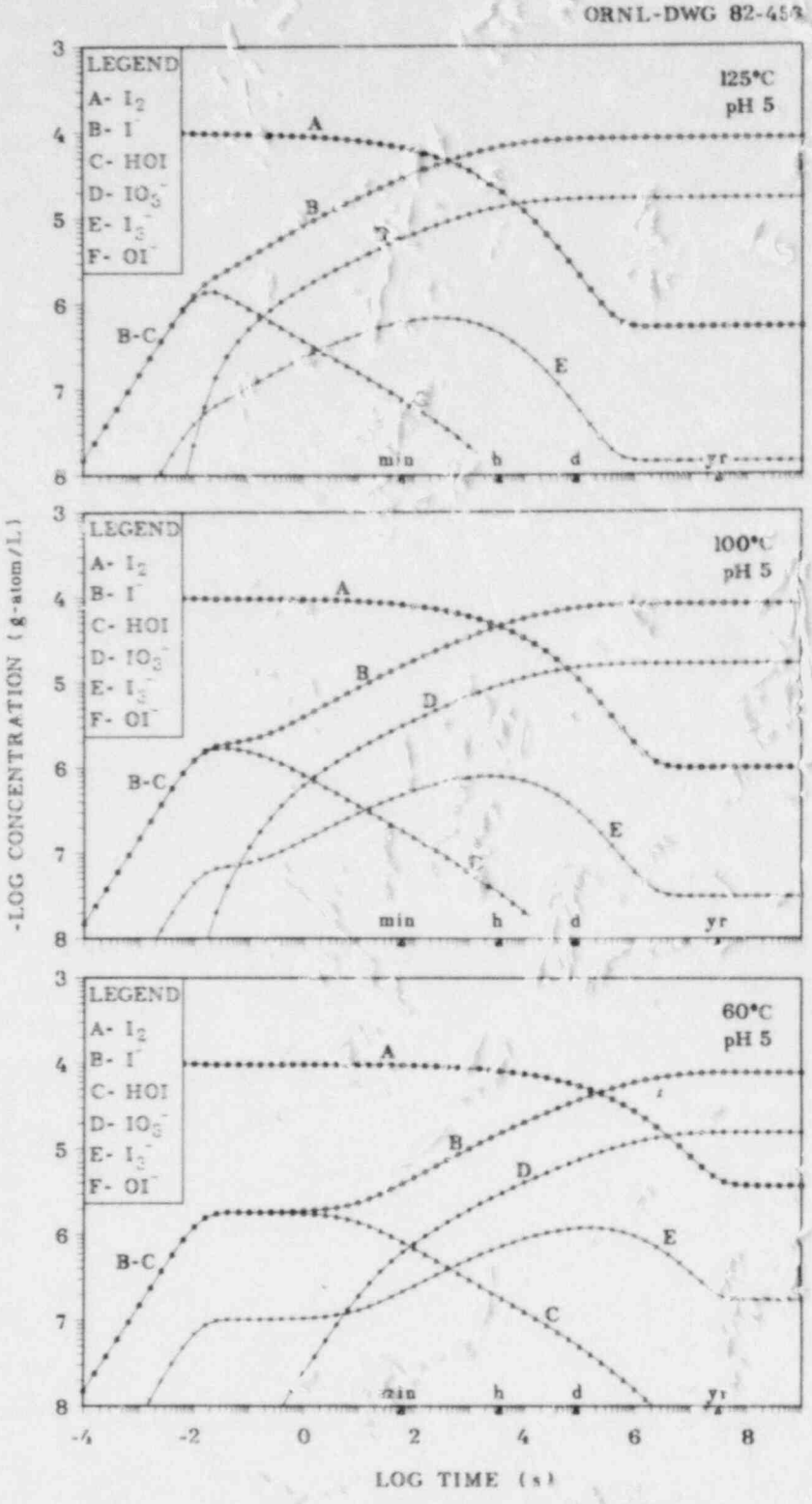

Fig. 17. Concentrations of iodine species as a function of time when 10^{-4} g-atom/L of I_2 equilibrates in water at 60, 100, and 125°C with a buffered pH of 5.

ORNL-DWG 82-457

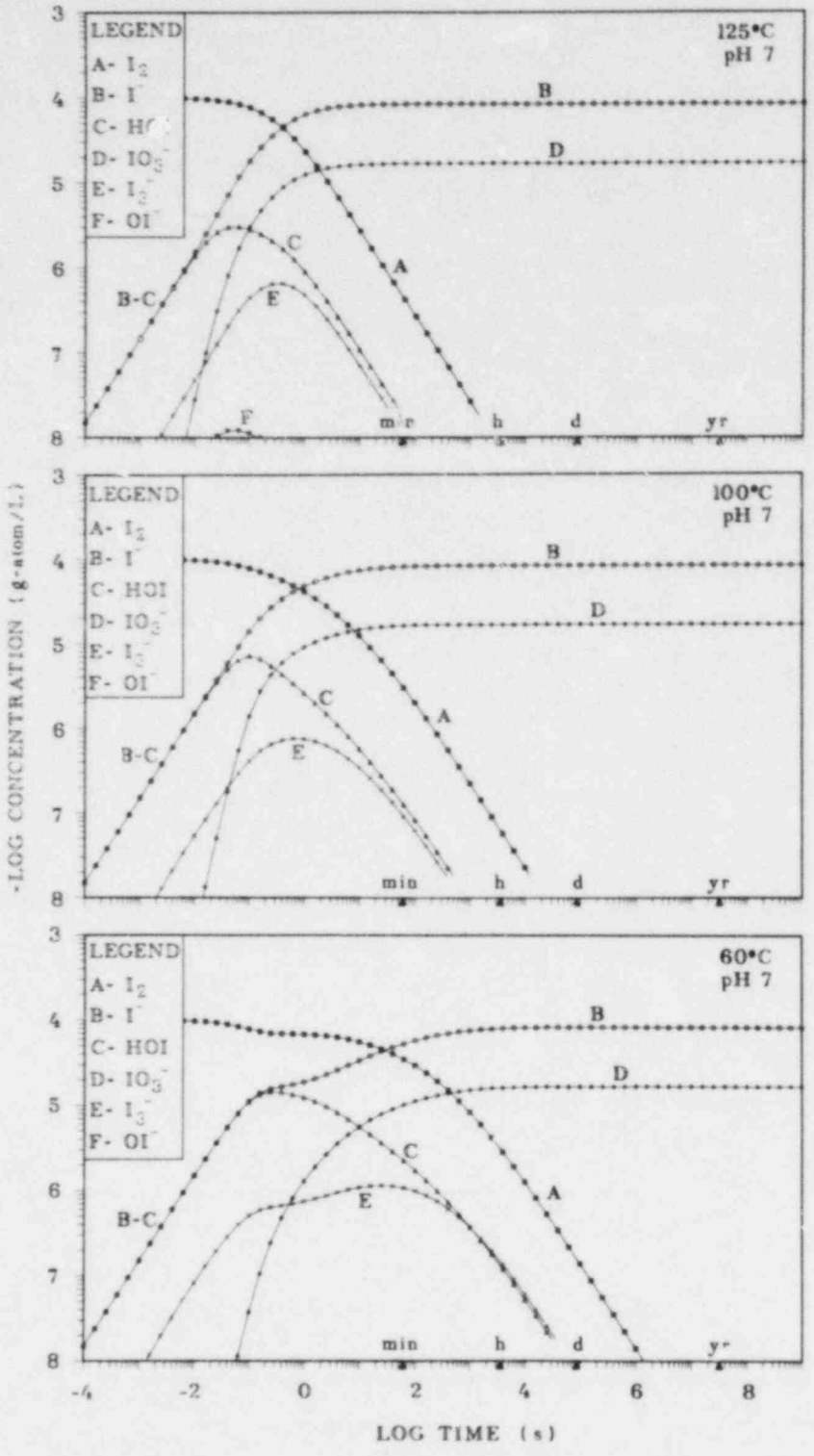

Fig. 18. Concentrations of iodine species as a function of time when 10^{-4} g-atom/L of I_2 equilibrates in water at 60, 100, and 125°C with a buffered pH of 7.

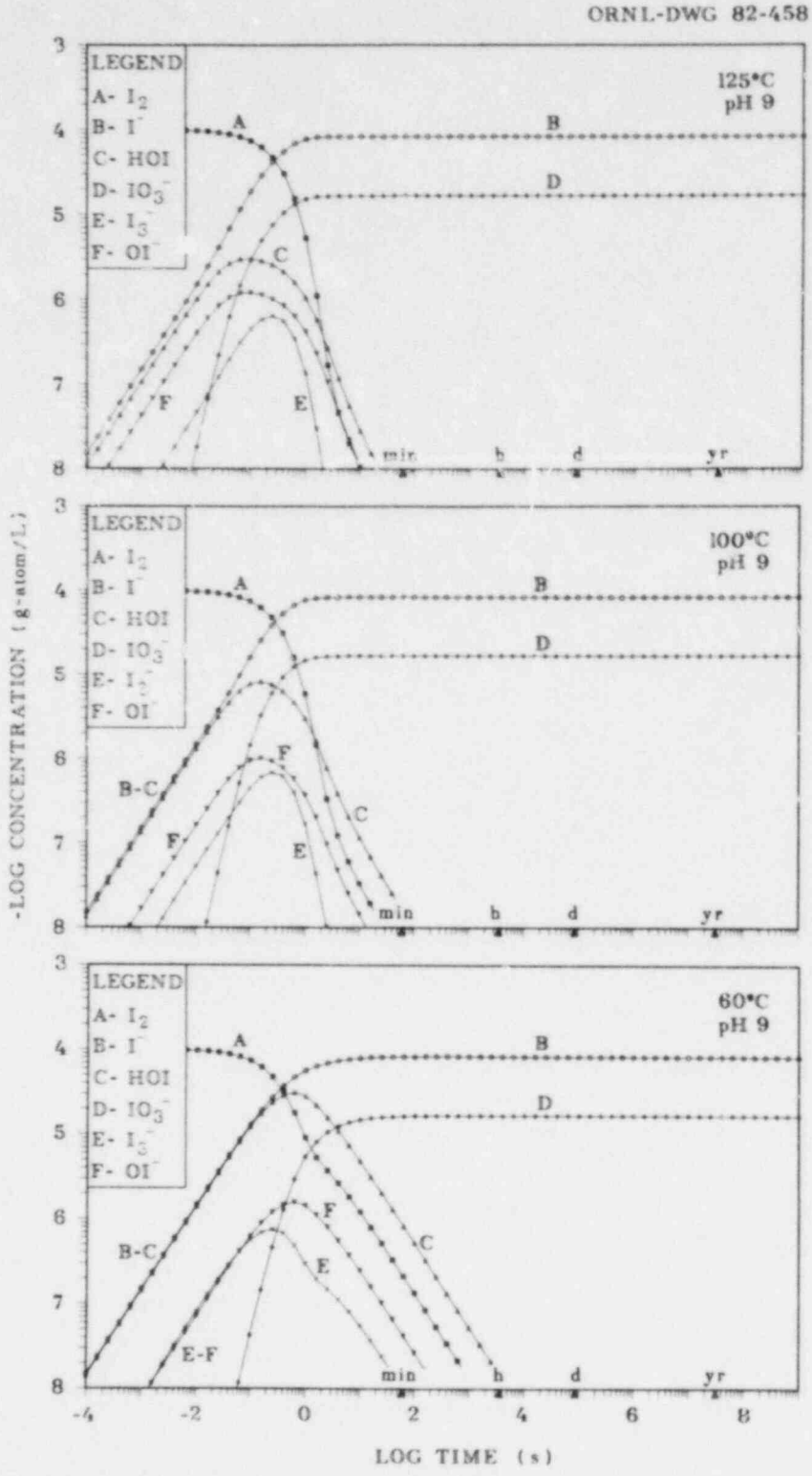

Fig. 19. Concentrations of iodine species as a function of time when 10^{-4} g-atom/L of I_2 equilibrates in water at 60, 100, and 125°C with a buffered pH of 9.

ORNL-DWG 82-459

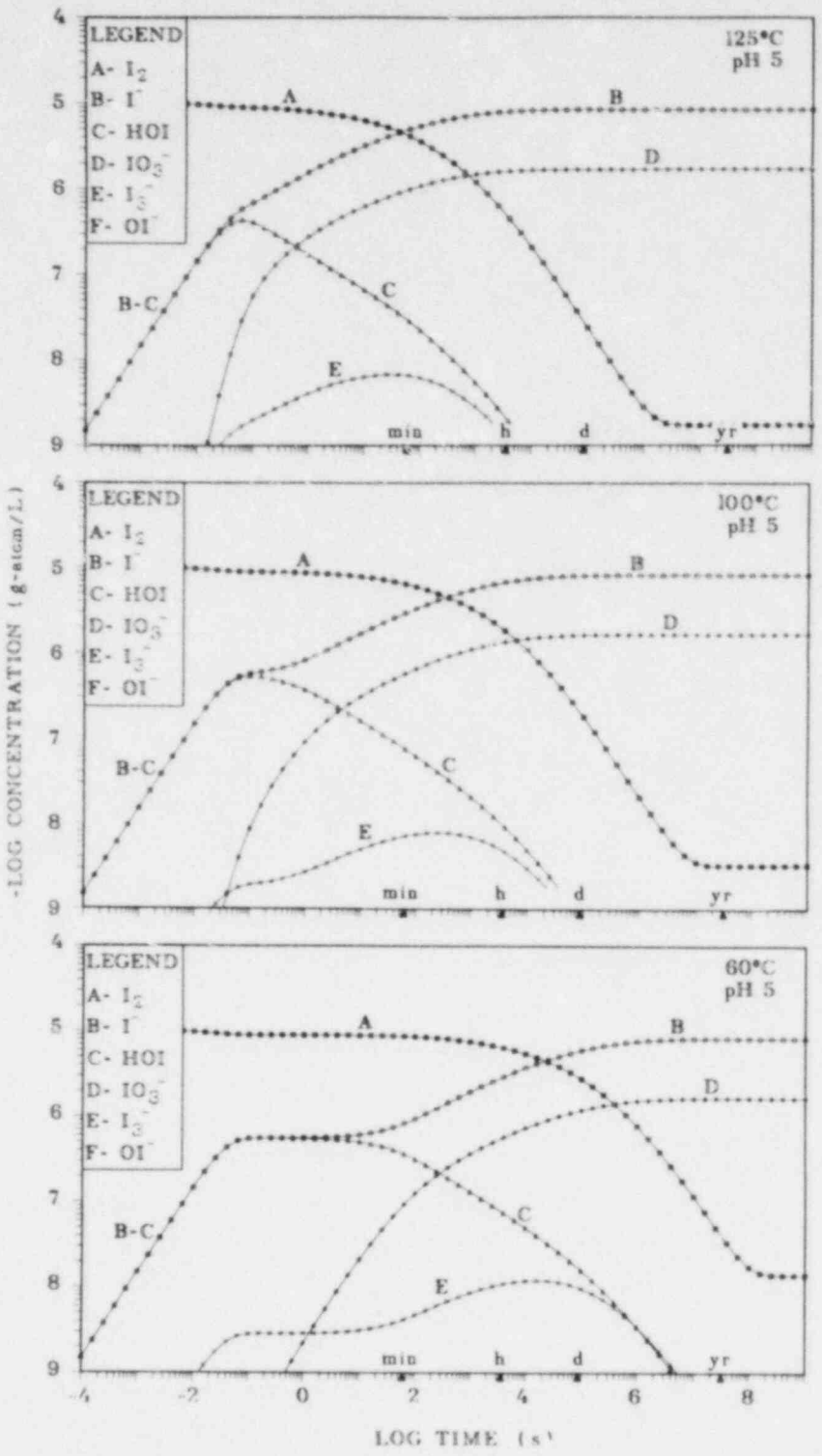

Fig. 20. Concentrations of iodine species as a function of time when 10^{-5} g-atom/L of I_2 equilibrates in water at 60, 100, and 125°C with a buffered pH of 5.

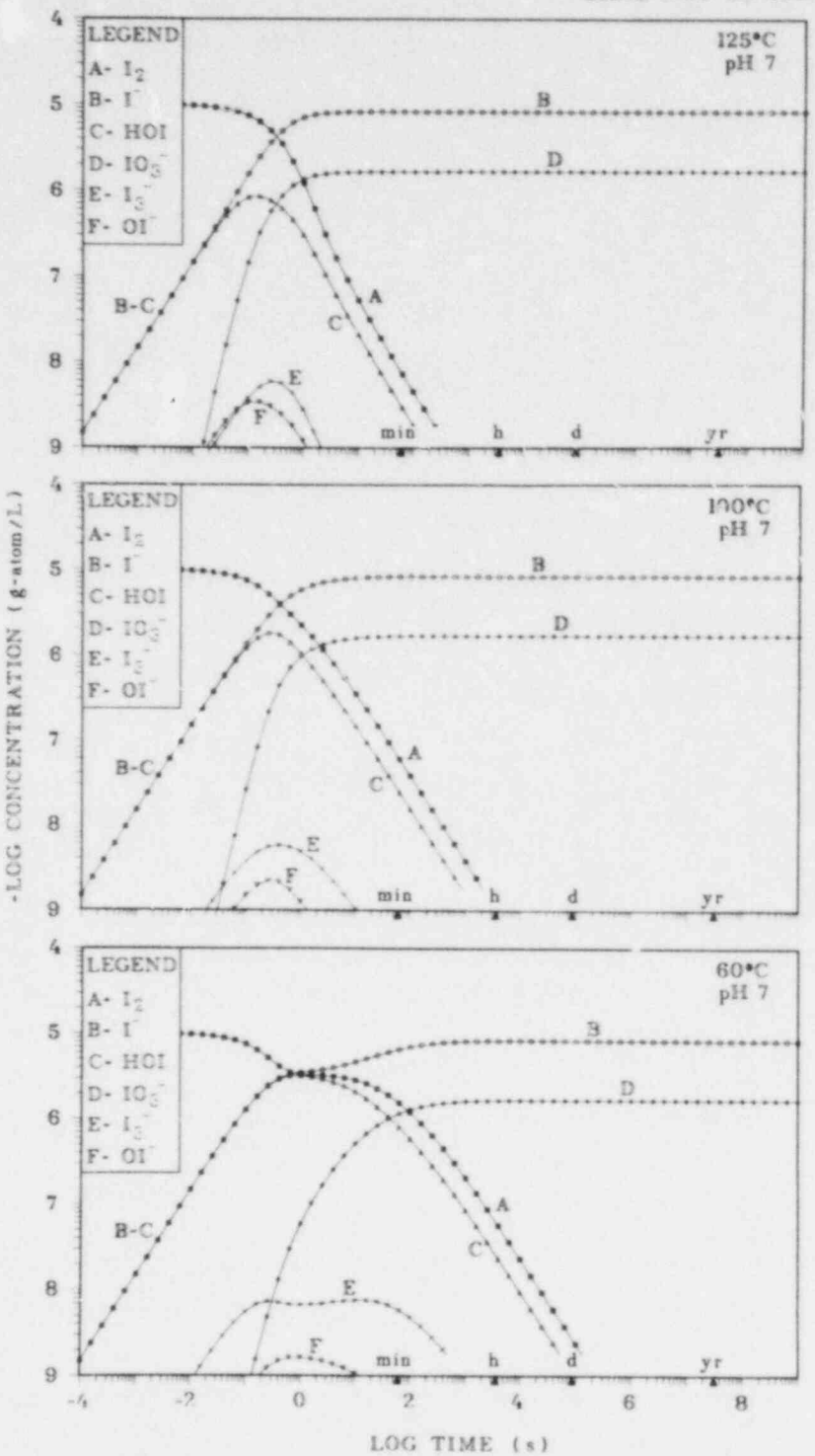

Fig. 21. Concentrations of iodine species as a function of time when 10^{-5} g-atom/L of I_2 equilibrates in water at 60, 100, and 125°C with a buffered pH of 7.

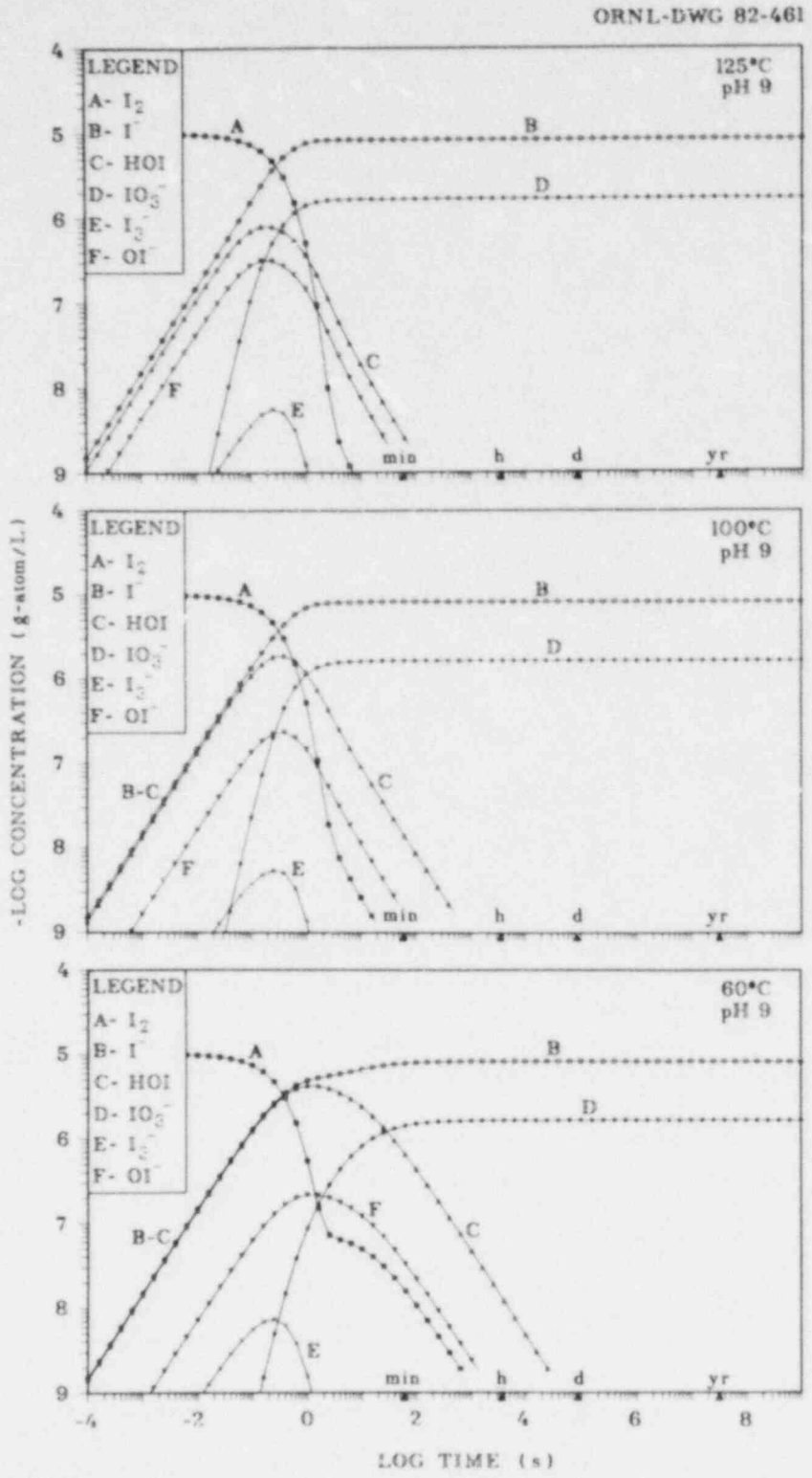

Fig. 22. Concentrations of iodine species as a function of time when 10^{-5} g-atom/L of I_2 equilibrates in water at 60, 100, and 125°C with a buffered pH of 9.

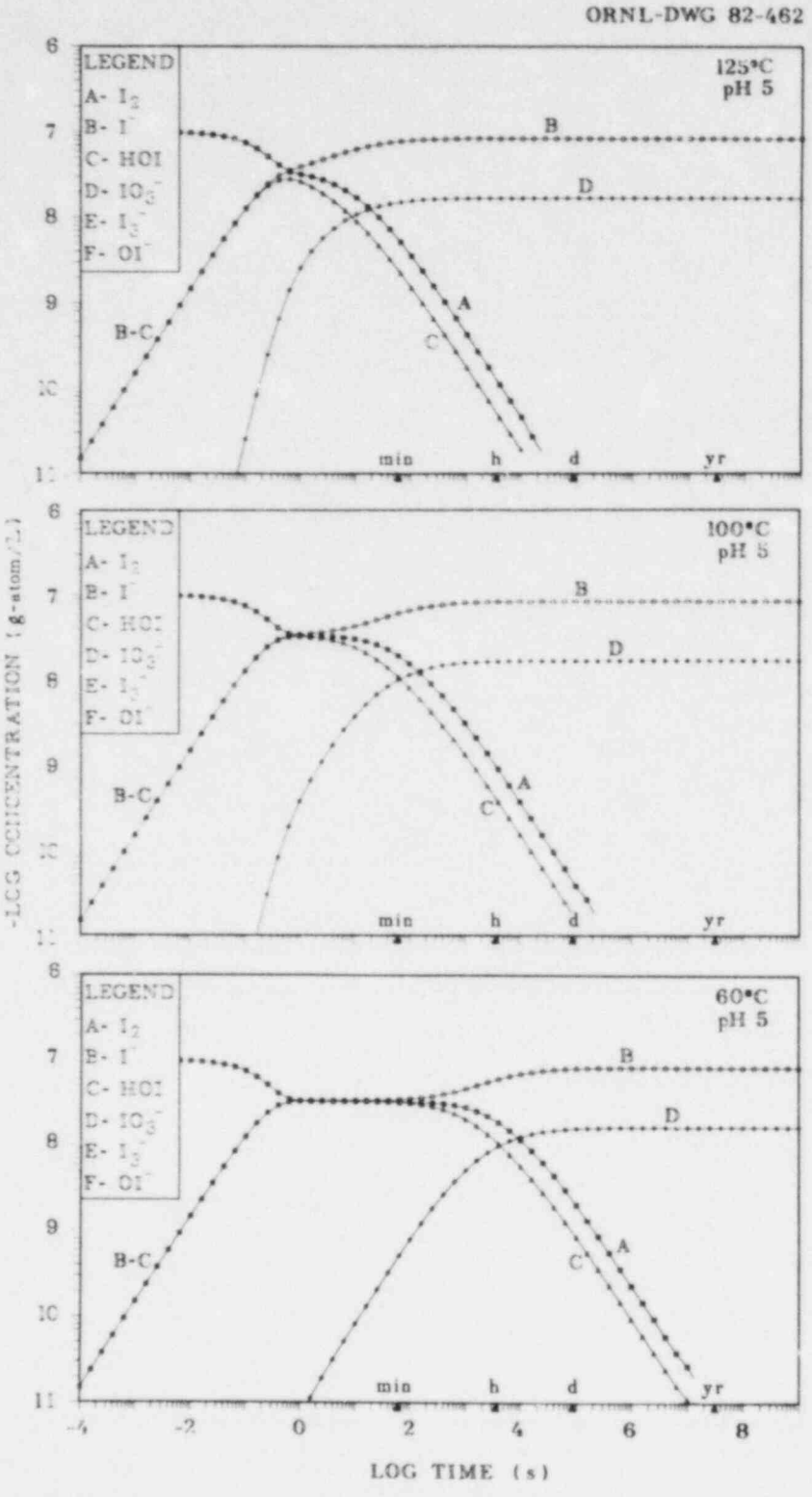

Fig. 23. Concentrations of iodine species as a function of time when 10^{-7} g-atom/L of I_2 equilibrates in water at 60, 100, and 125°C with a buffered pH of 5.

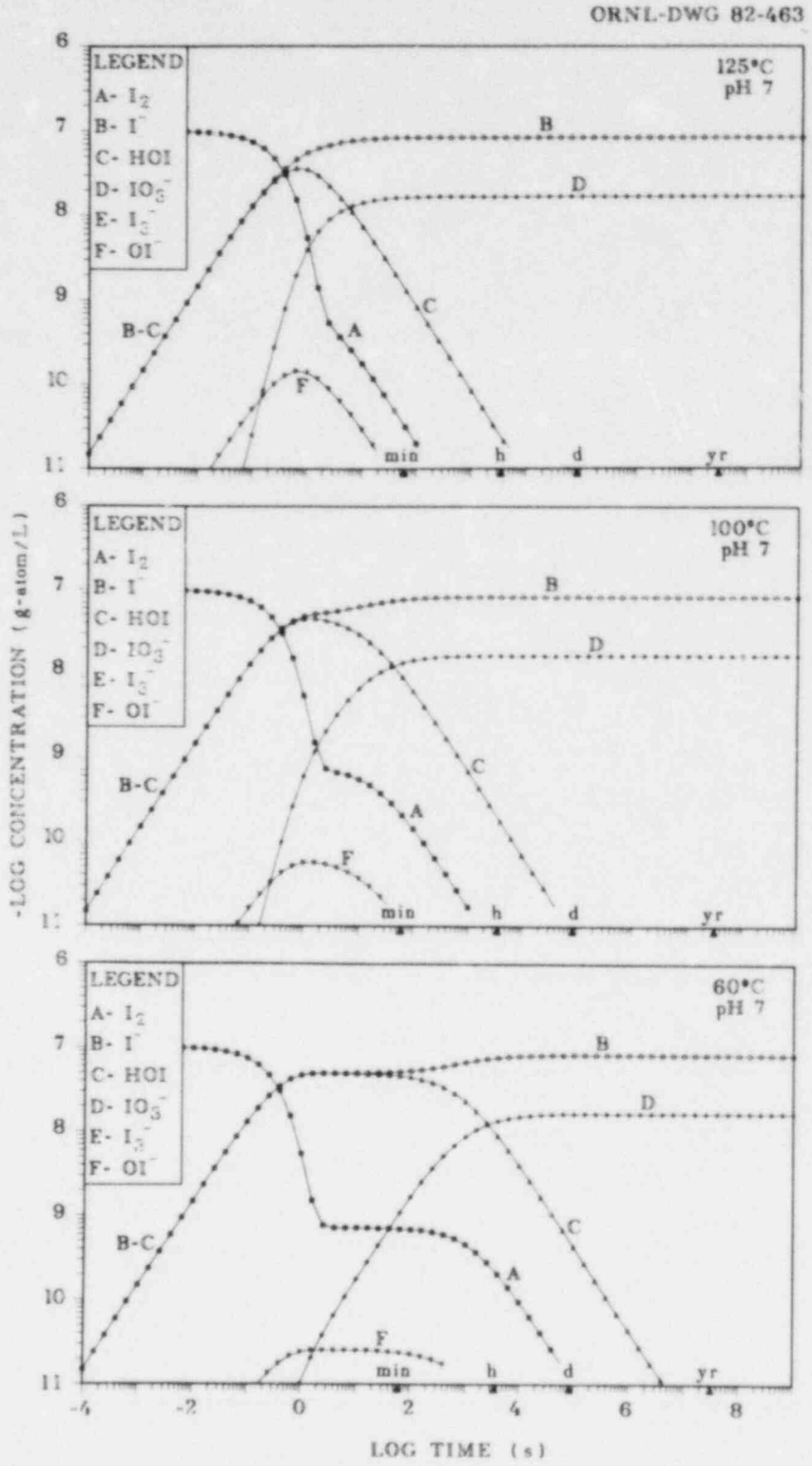

Fig. 24. Concentrations of iodine species as a function of time when 10^{-7} g-atom/L of I_2 equilibrates in water at 60, 100, and 125°C with a buffered pH of 7.

ORNL-DWG 82-464

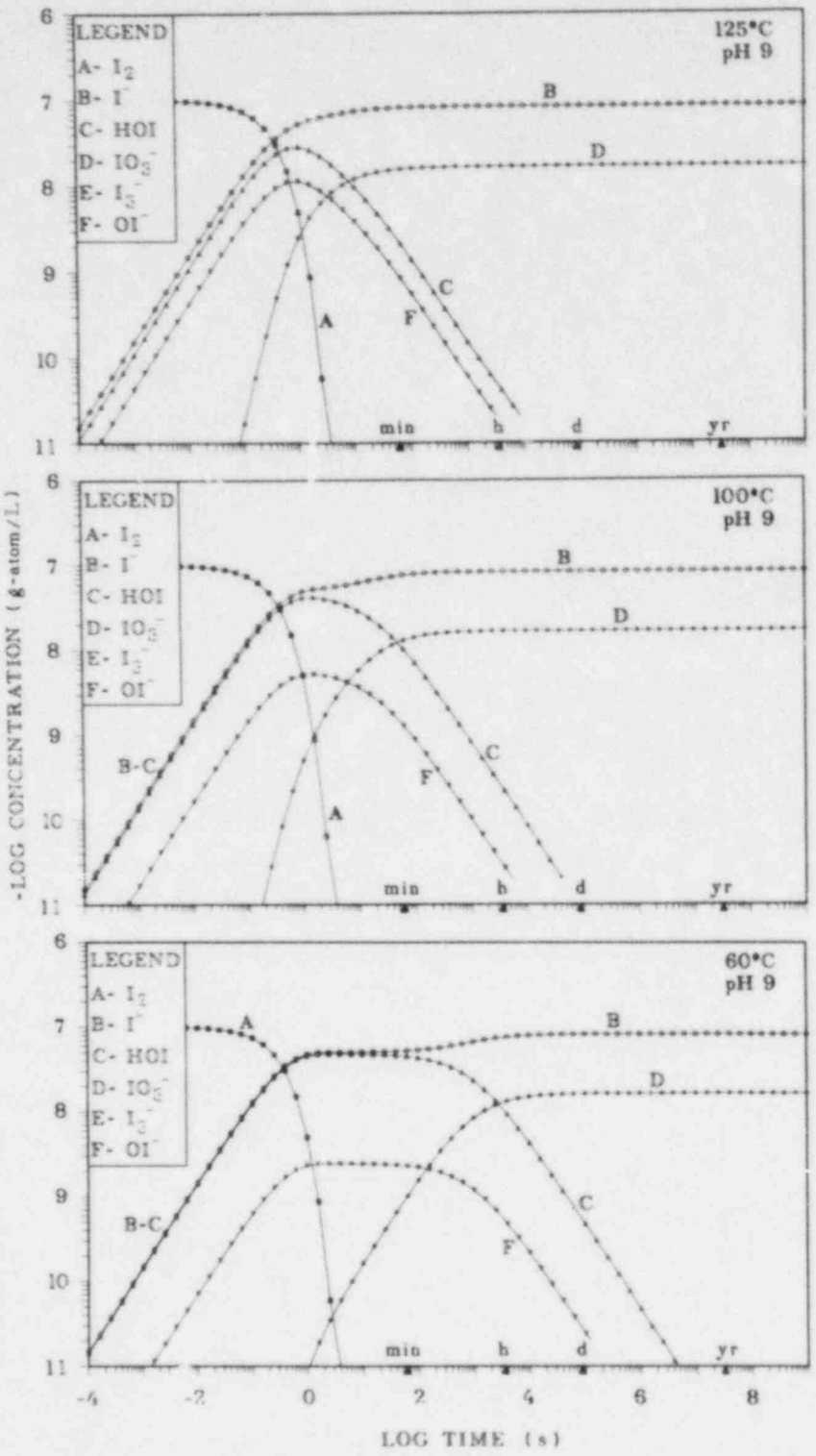

Fig. 25. Concentrations of iodine species as a function of time when 10^{-7} g-atom/L of I_2 equilibrates in water at 60, 100, and 125°C with a buffered pH of 9.

ORNL-DWG 82-485

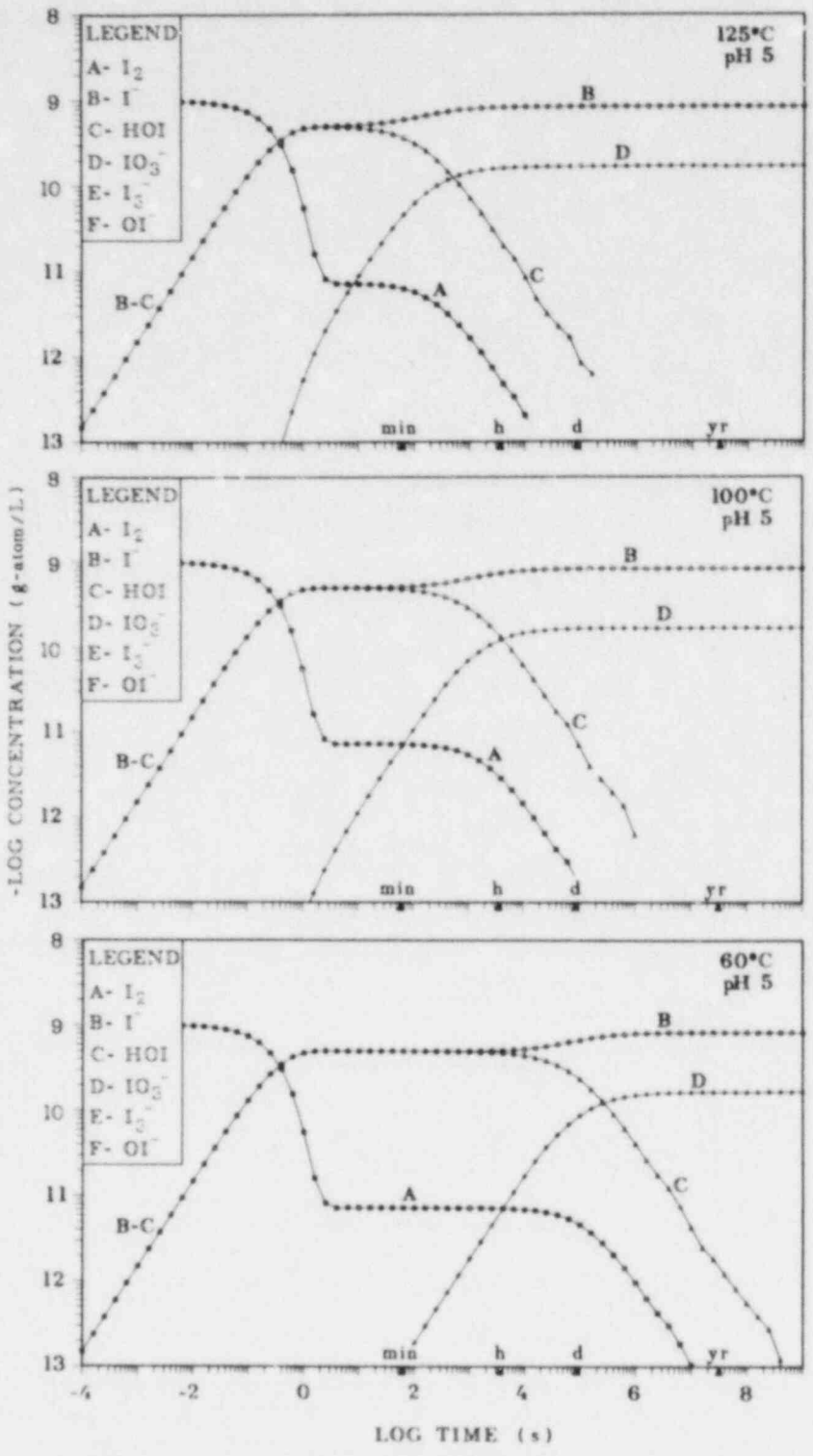

Fig. 26. Concentrations of iodine species as a function of time when 10^{-9} g-atom/L of I_2 equilibrates in water at 60, 100, and 125°C with a buffered pH of 5.

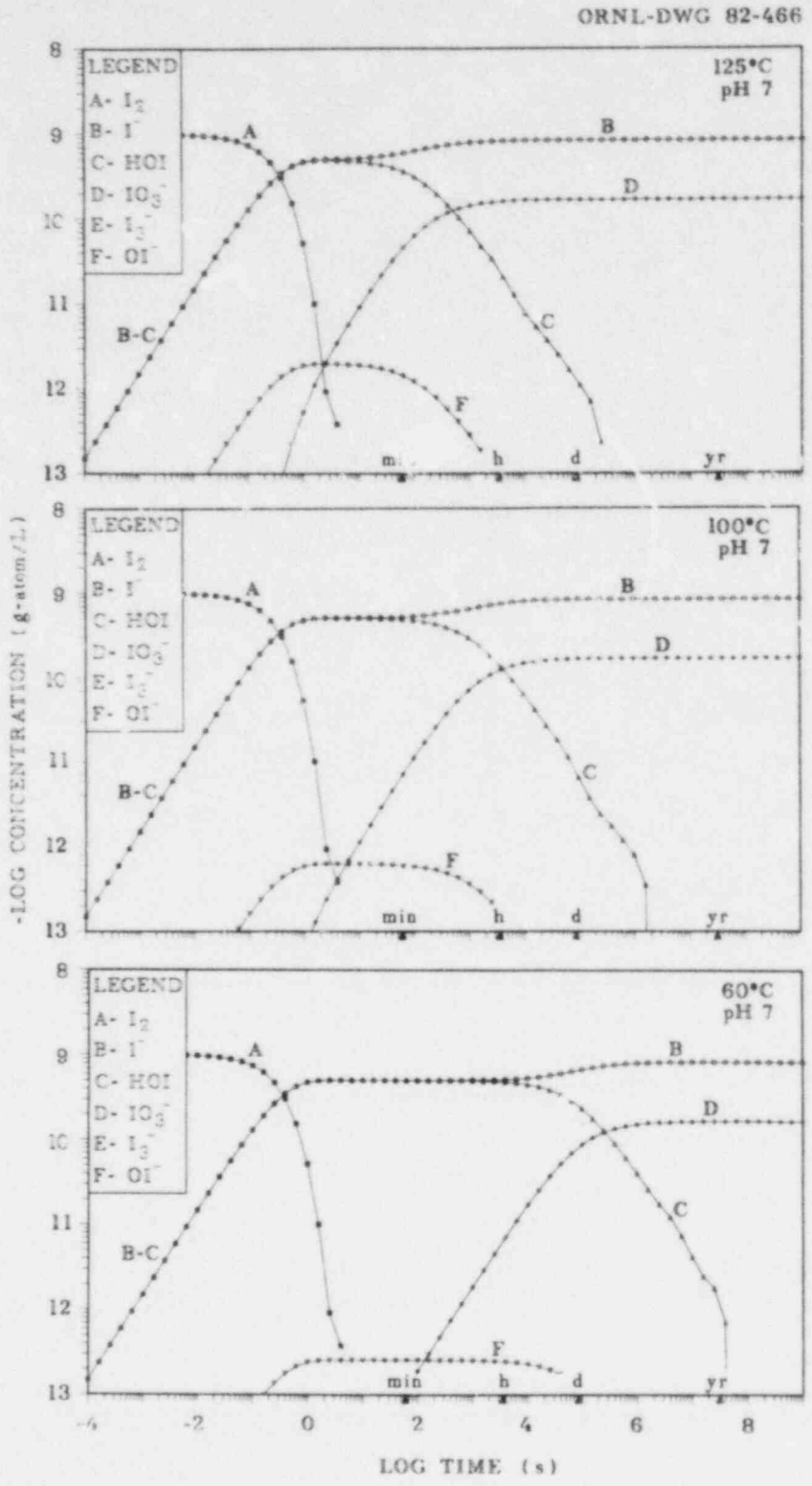

Fig. 27. Concentrations of iodine species as a function of time when 10^{-9} g-atom/L of I_2 equilibrates in water at 60, 100, and 125°C with a buffered pH of 7.

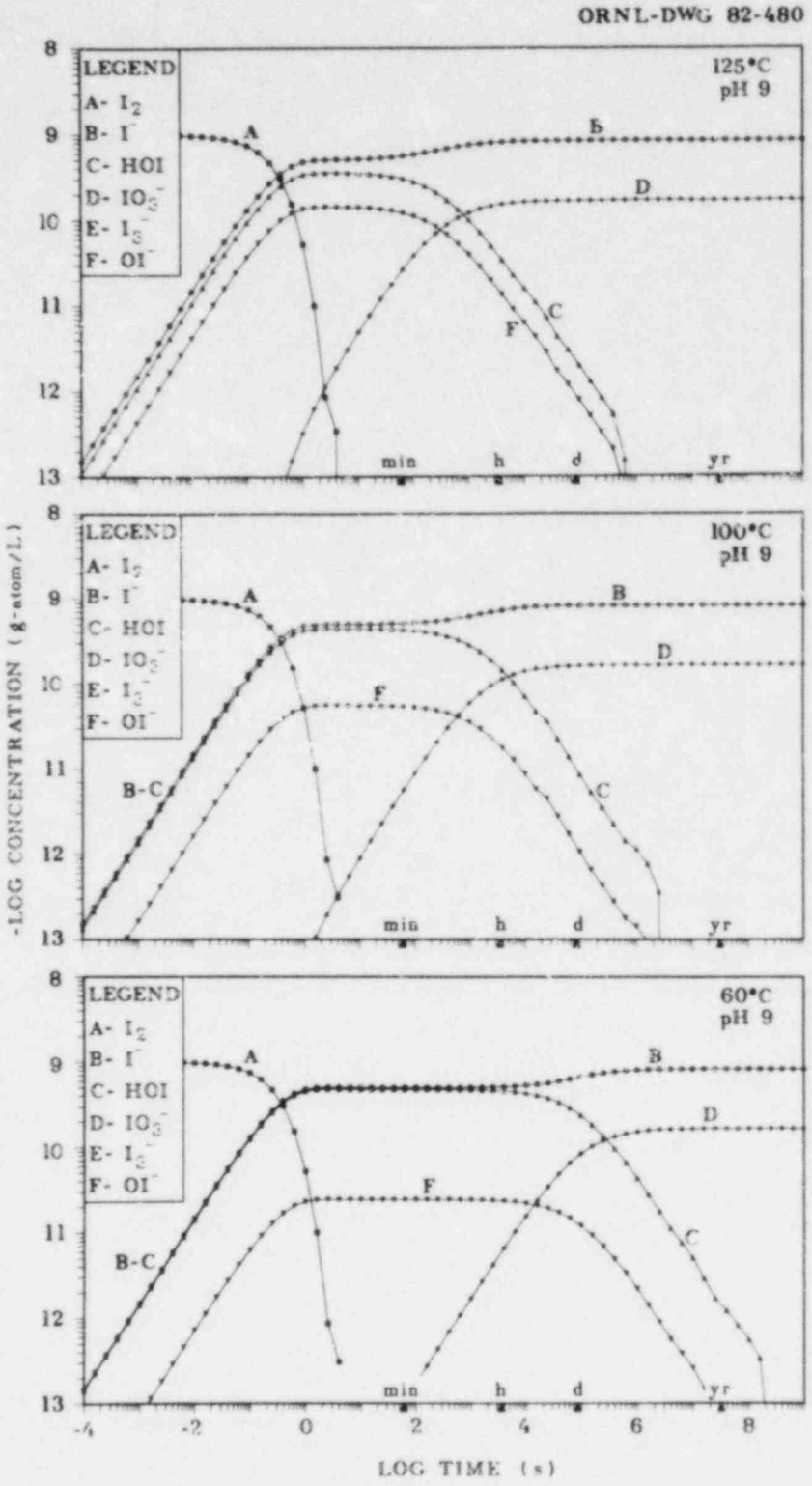

Fig. 28. Concentrations of iodine species as a function of time when 10^{-9} g-atom/L of I_2 equilibrates in water at 60, 100, and 125°C with a buffered pH of 9.

ORNL DWG 82-455

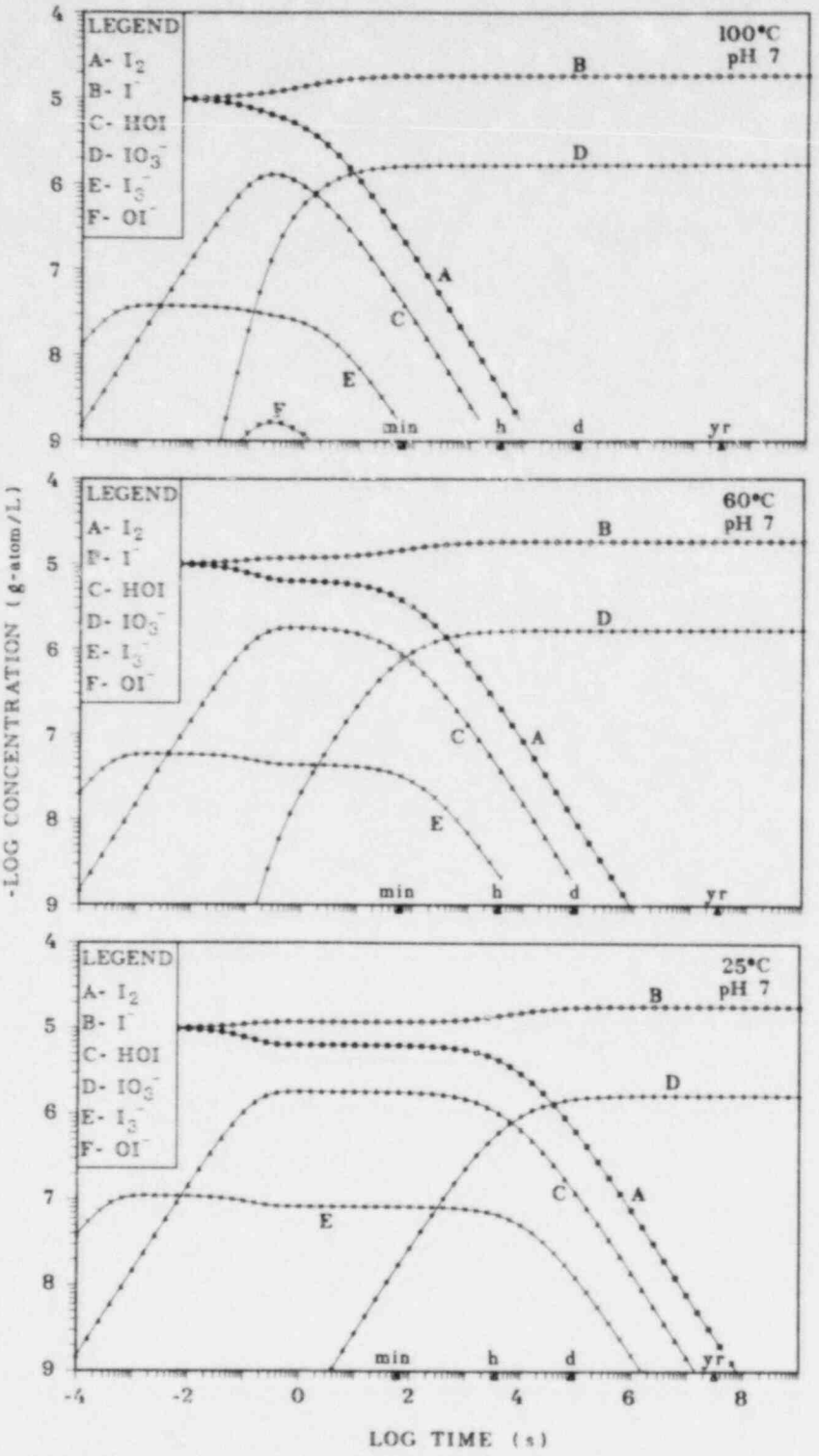

Fig. 29. Concentrations of iodine species as a function of time when 10^{-5} g-atom/L of I_2 and 10^{-5} g-atom/L of I^- equilibrates in water at 25, 100, and 125°C with a buffered pH of 7.

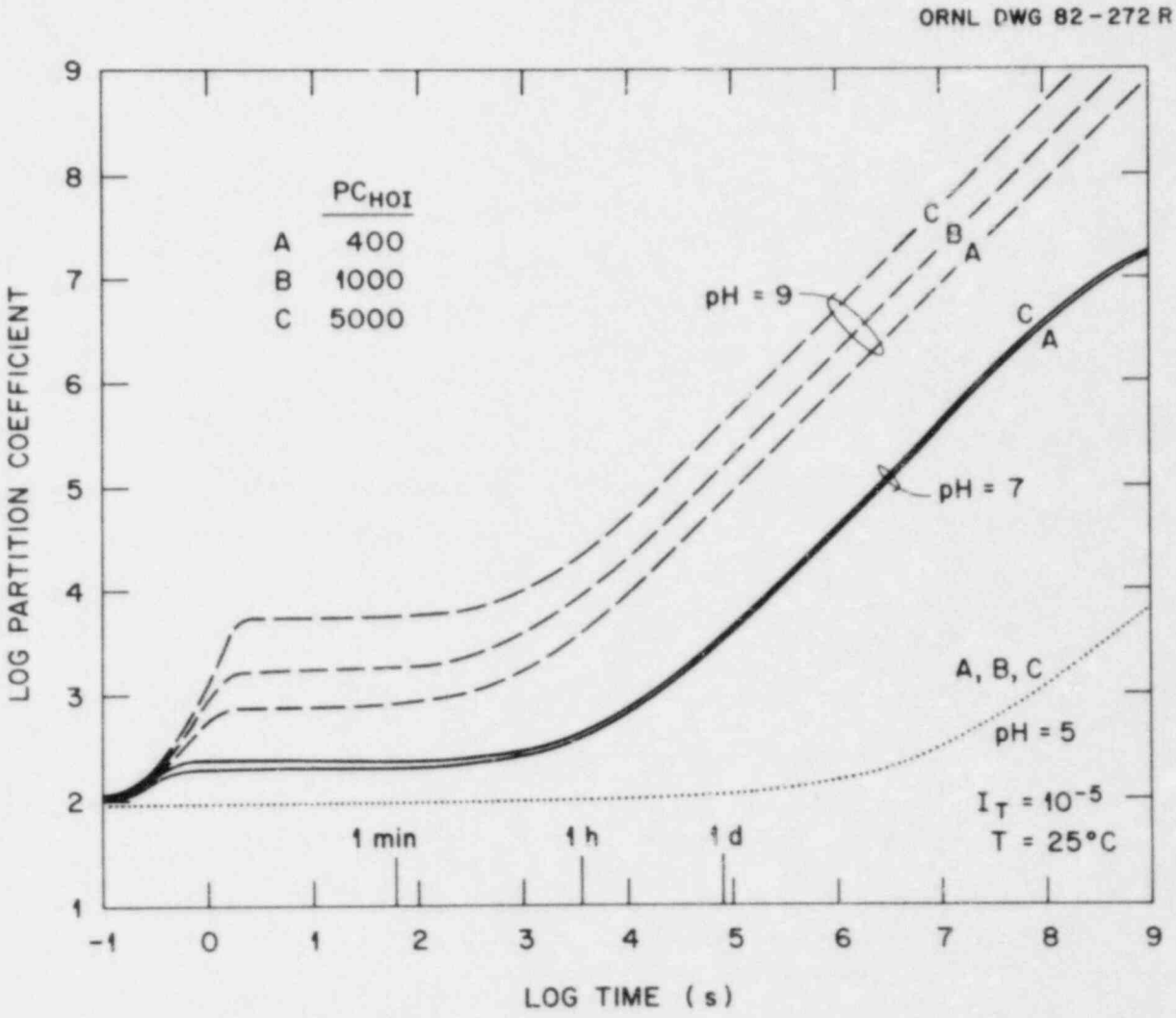

Fig. 30. Log-log plots of iodine partition coefficients vs time when 10^{-5} g-atom/L of I_2 equilibrates in water at 25°C with pH values of 5, 7, and 9. The individual partition coefficient for the I_2 species was assumed to be 83, while three estimates for HOI, 400, 1000, and 5000, were used.

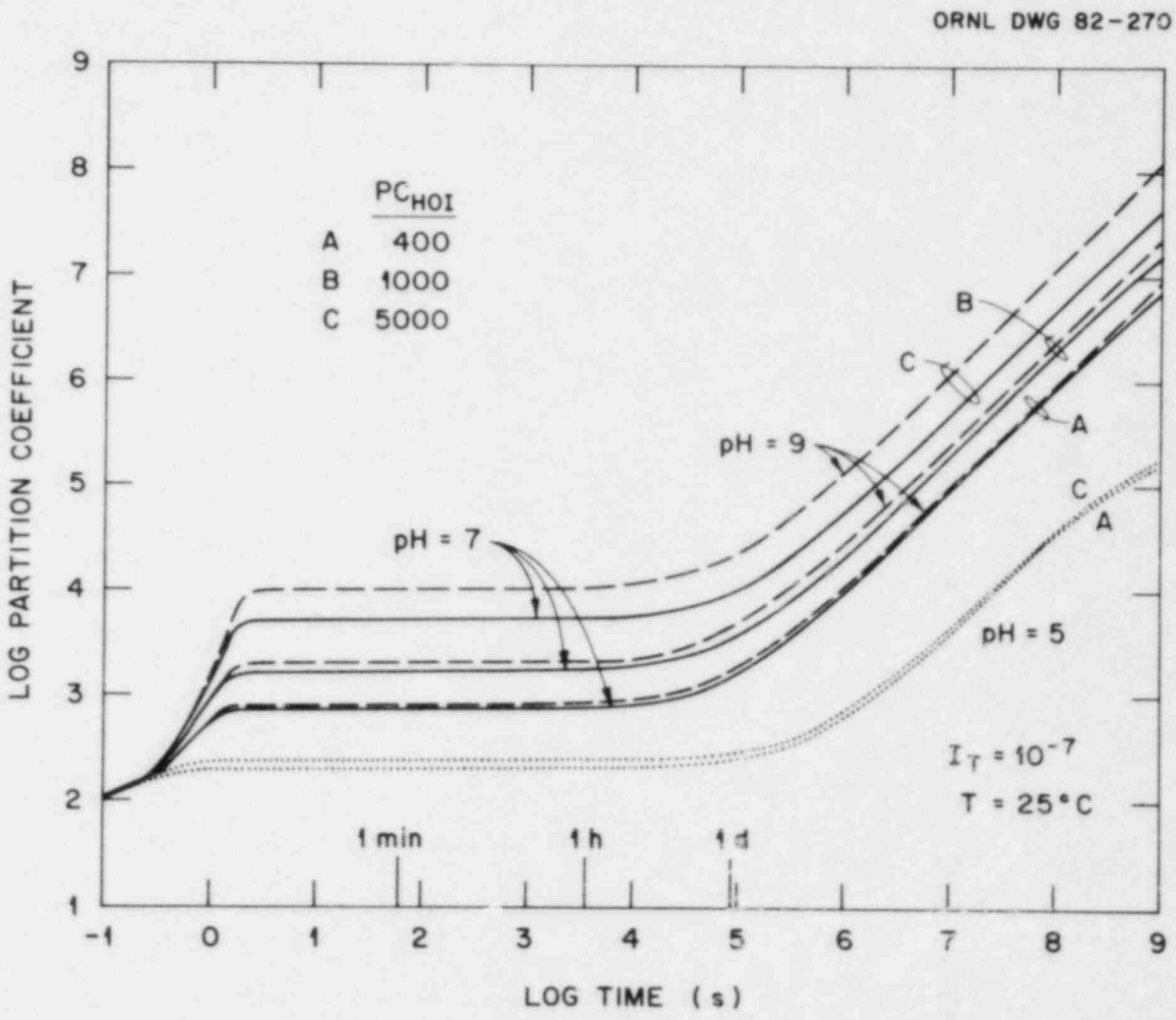

Fig. 31. Log-log plots of iodine partition coefficients vs time when 10^{-7} g-atom/L of I_2 equilibrates in water at 25°C with pH values of 5, 7, and 9. The individual partition coefficient for the I_2 species was assumed to be 83, while three estimates for HOI, 400, 1000, and 5000, were used.

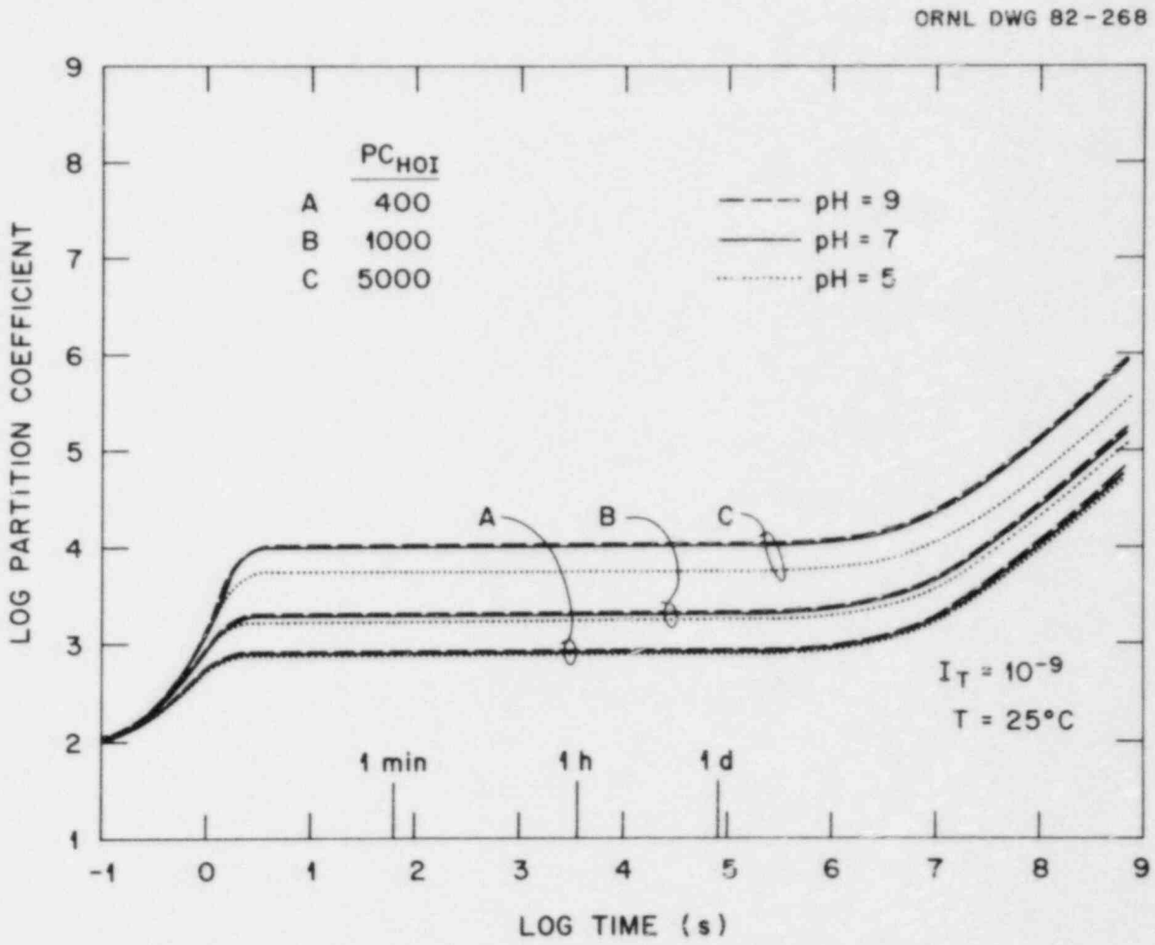

Fig. 32. Log-log plots of iodine partition coefficients vs time when 10^{-9} g-atom/L of I_2 equilibrates in water at 25°C with pH values of 5, 7, and 9. The individual partition coefficient for the I_2 species was assumed to be 83, while three estimates for HOI, 400, 1000, and 5000, were used.

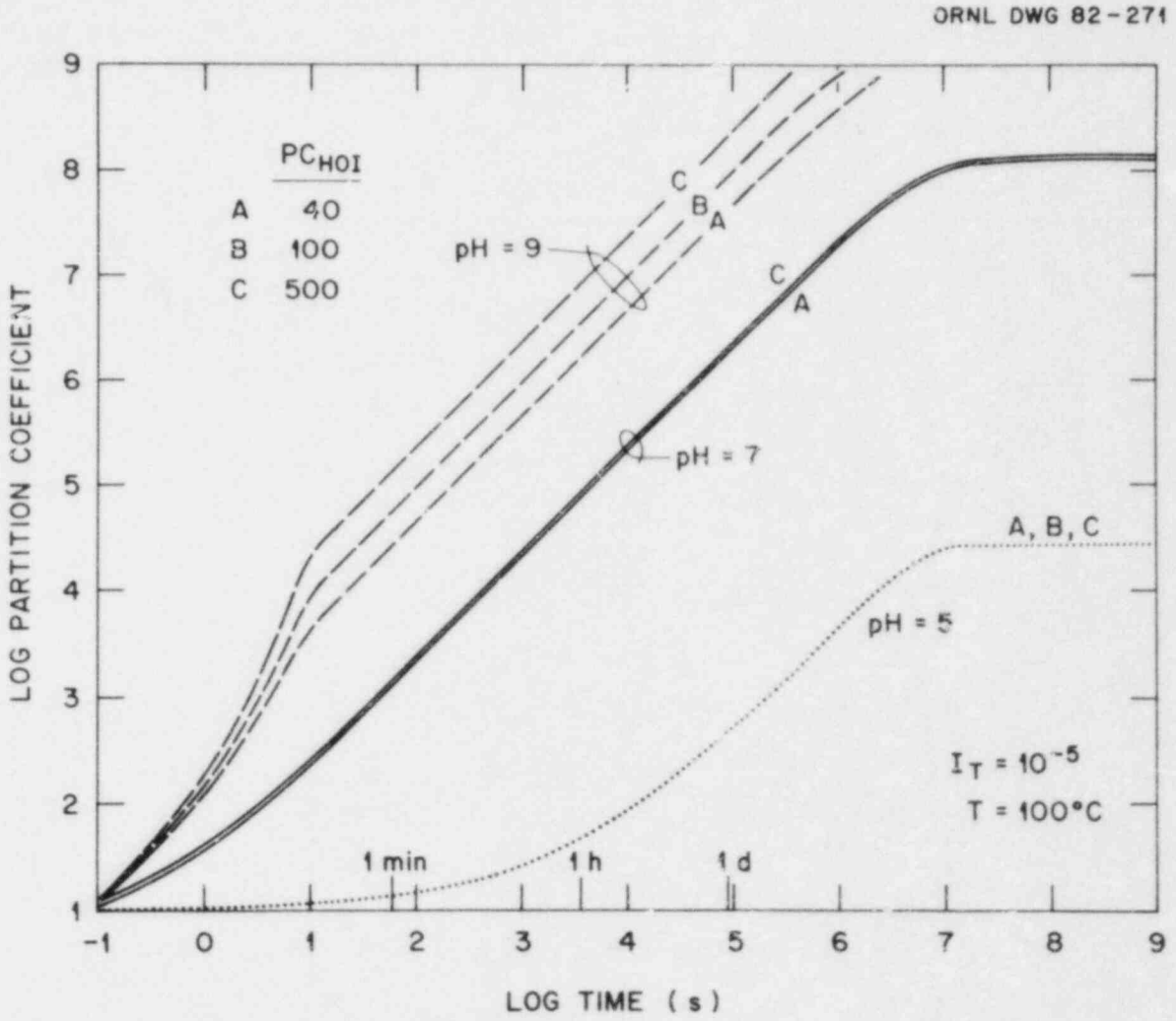

Fig. 33. Log-log plots of iodine partition coefficients vs time when 10^{-5} g-atom/L of I_2 equilibrates in water at 100°C with pH values of 5, 7, and 9. The individual partition coefficient for the I_2 species was assumed to be 9.1, while three estimates for HOI, 40, 100, and 500, were used.

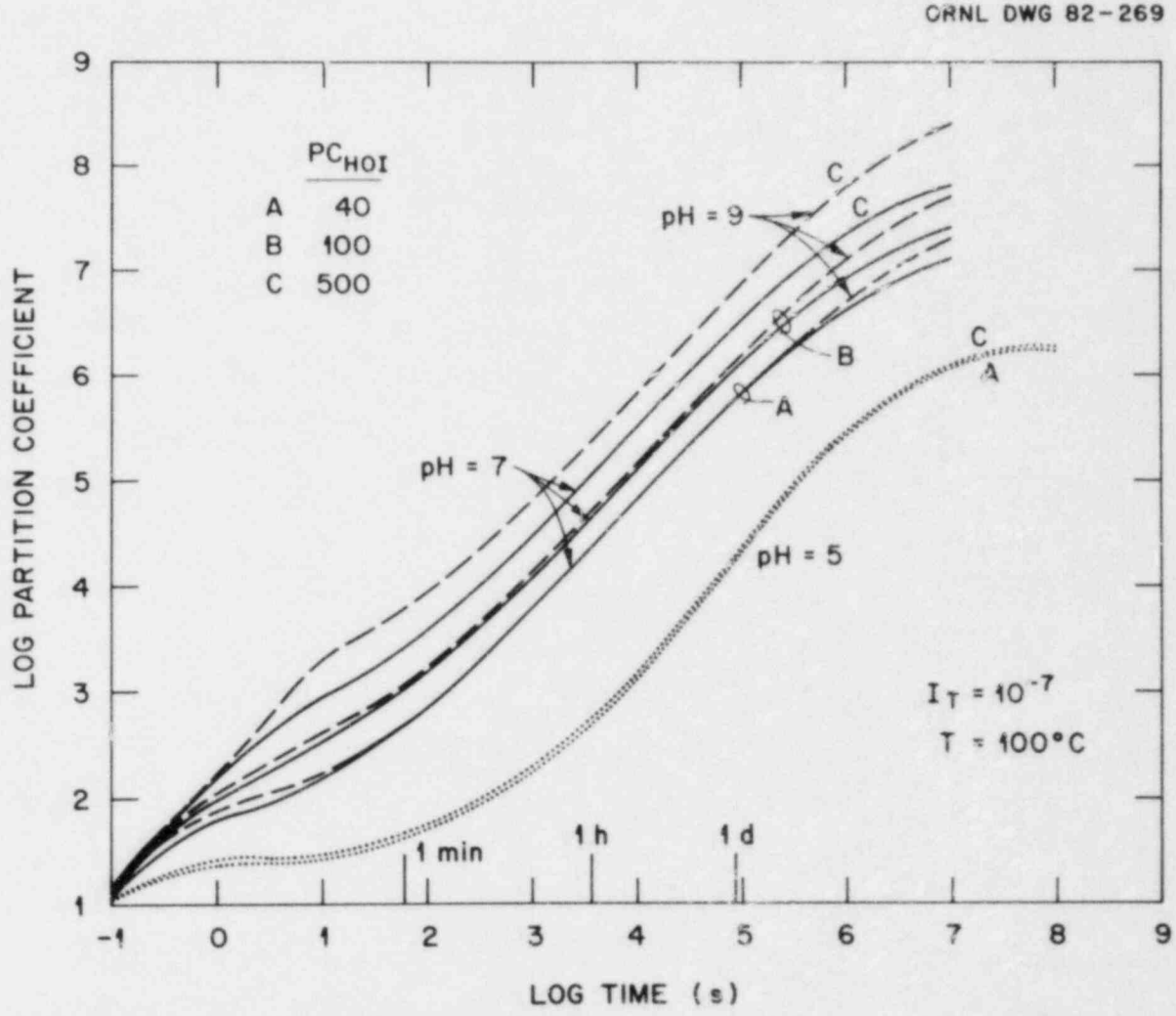

Fig. 34. Log-log plots of iodine partition coefficients vs time when 10^{-7} g-atom/L of I_2 equilibrates in water at 100°C with pH values of 5, 7, and 9. The individual partition coefficient for the I_2 species was assumed to be 9.1, while three estimates for HOI, 40, 100, and 500, were used.

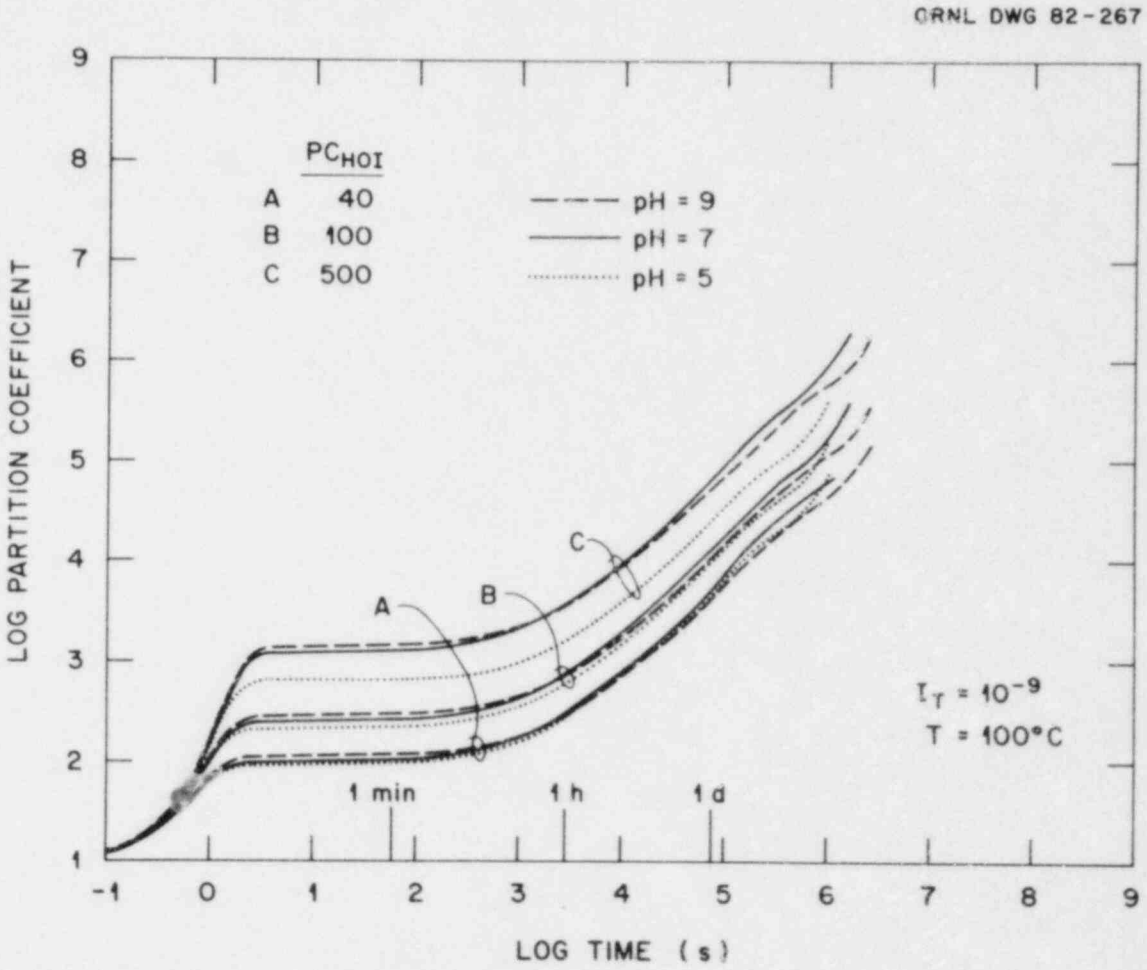

Fig. 35. Log-log plots of iodine partition coefficients vs time when 10^{-9} 100°C with pH values of 5, 7, and 9. The individual partition coefficient for the I_2 species was assumed to be 9.1, while three estimates for HOI, 40, 100, and 500, were used.

6. APPENDIX: COMPUTER PROGRAM IRATE

A listing of the FORTRAN program that simultaneously calculates the concentrations of six iodine species at each time interval following the hydrolysis of molecular iodine is given here. All the variables are input on the first two cards according to the format shown in Table A-1. These are followed in each case by 13 cards related to the plotting subroutine and are described below. A blank card following the last case terminates the calculations.

Definitions for the KIPLOT subroutine are as follows:

Third card:	title of the plot	
Fourth card:	XMIN	- time value at the origin on the x-axis
	DEX	- length in inches of each logarithm decade
	MAX	- final time value
	YMIN	- concentration value at the origin on the y-axis
	DEY	- length in inches of each logarithm decade
	YMAX	- maximum concentration value
Fifth card:	XLEG	- distance in inches of the left-hand side of the legend box from the origin along the x-axis
	YLEG	- distance in inches from the bottom of the legend box from the origin along the y-axis
	XILEG	- width in inches of the legend box
	XLEN	- maximum length of title in inches

The format for the fourth and fifth cards pertaining to the plotting subroutine is also given in Table A-1. The remaining ten cards contain the DISSPLA code for the iodine species shown in the legends on the figures. More details of this code and the DISSPLA package, in general, are available in DISSPLA Manual, Volume 1.

The contents of the various cards can be summarized as follows:

Card No.	Content
1-2	Variables
3-5	KIPLOT subroutine
6-15	DISSPLA code
16	Blank

Table A-1. Input data

Card No.	Field	Variable	Format
1[a]	1-10	RKI	E10.0
	11-20	RKM1	E10.0
	21-30	RK20	E10.0
	31-40	RK21	E10.0
	41-50	RKM2	E10.0
	51-60	RKM3	E10.0
	61-70	RKP4	E10.0
2[b]	1-10	PH	E10.0
	11-20	EMO	E10.0
	21-30	N	I10
	31-40	TC	E10.0

[a]The variables represented by RK1 through RKP4 correspond to the rate constants k_1, k_{-1}, k_{20}, k_{21}, k_{-2}, K_{-3}, and k_{p4}, respectively. The variables EKI3, EKHOI, and EKW, which are included in the program, refer to the equilibrium constants K_3, K_2, and K_w, respectively.

[b]The remaining input variables (on card 2) are defined as follows:

PH - pH of the solution,
EMO - the initial iodine concentration,
N - number of timesteps to be calculated,
TC - temperature in degrees Celsius.

```
C      KINETICS OF IODINE HYDROLYSIS
       IMPLICIT REAL*8(A-H,O-Z)
       DIMENSION Y(10),YI(10),YN(10),YP(10),YO(10),YNNN(150,10),
      1K1(10),K2(10),K3(10),K4(10),K5(10),P(10),R(10),P1(10),IPAR(800),LA
      2B(10),XTIME(150)
       DIMENSION ATOL(10),RWORK(92),IWORK(25)
       EXTERNAL FEX,JEX
       COMMON /D/ RK1,RKM1,RK20,RK21,RKM2,EKI3,EKHOI,EKW,PH,HCON,
      1RK3,SKM3,RKP4,XTIME,YNNN,YC
C
       PCHOI1(Y)=10.**(4220.46/Y-19.2546+0.02583*Y)
       PCHOI2(Y)=10.**(4220.46/Y-18.8567+0.0258?*Y)
       PCHOI3(Y)=10.**(4220.46/Y-18.1577+0.02583*Y)
C
C    RATE CONSTANTS ARE, RK1 AND RKM1 FOR THE REACTION   I2 + H2O = HOI + I- + H+
C    RATE CONSTANTS ARE, RK2O, RK21 AND RKM2 FOR THE REACTION ,
C    3HOI = IO3- + 2I- + 3H+
C
C
   50 READ 1,RK1,RKM1,RK20,RK21,RKM2,RKM3,RKP4
    1 FORMAT(8E10.0)
      IF(RK1 .EQ. 0.) CALL EXIT
C
C
C    PH = PH OF THE SOLUTION
C    EMO = THE INITIAL CONCENTRATION OF IODINE
C
C
      READ 2,PH,EMO,R,TC,EMPC
    2 FORMAT(2E10.0,I10,2E10.0)
C
C
C    EKI3 = EQUILIBRIUM CONSTANT FOR THE REACTION,  I2 + I- = I3-
C    EKHOI = EQUILIBRIUM CONSTANT FOR THE REACTION, HOI = H+ + OI-
C    EKW = EQUILIBRIUM CONSTANT FOR THE REACTION,  H2O = H+ + OH-
C
C
      TK=TC+273.15
      IF(TC.NE.25.)RK21=0.
      RKM2=1.47351D03/TK+2.22530+4.42592D-02*TK
      RKM2=DEXP(RKM2)
      EKHOI=10.**(2800.48+0.7335*TK-80670./TK-1115.1*DLOG10(TK))
      DW=1.00017-2.36592D-05*TC-4.77122D-06*TC**2+8.27411D-09*TC**3
      EKW=10.0**(-4.098-3245.2/TK+2.2362D+05/TK**2-3.984D+07/TK**3+(13.9
     1157-1262.2/TK+8.5641D+05/TK**2)*DLOG10(DW))
      EKI3=DEXP(3727.86/TK-11.6326+0.0192212*TK)
      IF (TC.GT.112.)GO TO 1111
      PCI2=10.**(4220.46/TK-19.9905+0.02583*TK)
      GO TO 1112
 1111 PCI2=10.**(5615.40/TK-25.1790+0.02990*TK)
 1112 CONTINUE
      RK3=EKI3*RKM3
      Y(1)=EMO
      DO 10 I=2,10
   10 Y(I)=0.D0
      Y(2)=EMMO
```

```
      T)=EMC
      HCON=10**(-PH)
      PRINT 6,PH,TC
    6 FORMAT(1H1,10X,'PH ='CPF5.1,10X,'TEMP. =',F6.1,' DEG. C')
      NEQ=5
      T=0.D0
      TOUT=1.D-4
      ITOL=2
      RTOL=1.D-4
      ATOL(1)=1.D-12
      ATOL(2)=1.D-8
      ATOL(3)=1.D-12
      ATOL(4)=1.D-8
      ATOL(5)=1.D-12
      ITASK=1
      ISTATE=1
      IOPT=0
      IRW=92
      LIW=25
      MF=21
      PRINT 5
    5 FORMAT(1H0,4X,'TIME',9X,'I2',8X,'IODIDE',8X,'HOI',7X,'IODATE',5X,
     1'TRIIODIDE',2X,'HYPOICDITE',3X,'I-BALANCE',3X,'PC(1)',5X,'PC(2)',5
     2X,'PC(3)',)
      DO 3 I=1,7
    3 YO(I)=Y(I)
      YO(1)=2.D0*Y(1)
      YO(7)=2.D0*Y(7)+Y(2)
      PRINT 4,T,(YO(I),I=1,10)
    4 FORMAT(1H0,1PE11.3,7E12.3,3E10.2)
      DO 40 IOUT=1,M
      CALL LSODE(FEX,NEQ,Y,T,TOUT,ITOL,RTOL,ATOL,ITASK,ISTATE,IOPT,RWORK
     1,IRW,IWORK,LIW,JEX,MF)
      DO 11 I=1,5
   11 YN(I)=Y(I)
      YN(6)=EKHOI*YN(3)/(HCON+EKHOI)
      YN(7)=YN(1)+0.5*(YN(2)+YN(3)+YN(4))
C
C   CONVERSION TO GATOM/L FROM MOLES/L
C
  301 YO(1)=YN(1)*2.D0
      YO(2)=YN(2)
      YO(3)=(YN(3)-YN(6))
      YO(4)=YN(4)
      YO(5)=YN(5)*3.0D0
      YO(6)=YN(6)
      YO(7)=YN(7)*2.D0
      L=8
      DO 123 K=1,3
      IF(K.EQ.1)PCP=PCHOI1(TK)
      IF(K.EQ.2)PCP=PCHOI2(TK)
      IF(K.EQ.3)PCP=PCHOI3(TK)
      YO(L)=YO(7)/(YO(1)/PCI2+YO(3)/PCP)
      L=L+1
  123 CONTINUE
      DO 42 J=1,6
```

```
      IF (YC(J).LT.0.)YC(J)=1.D-40
   42 CONTINUE
  200 PRINT 4,TOUT,(YC(I),I=1,10)
      XTIME(ICUT)=TOUT
      TP=DLOG10(TOUT)
      DPC=TP+0.2
      TOUT=10.**DEC
      DO 202 J=1,6
  202 YMAN(ICUT,J)=YC(J)
      IF(ISTATE .LT. 0) GO TO 80
   40 CONTINUE
      PRINT 60,IWORK(11),IWORK(12),IWORK(13)
   60 FORMAT(/12H NO. STEPS =,I4,11H  NO. F-S =,I4,11H  NO. J-S =,I4)
      CALL KIELOT(6,N)
      GO TO 50
  555 STOP
   80 PRINT 90,ISTATE
   90 FORMAT(///22H ERROR HALT.. ISTATE =,I3)
      STOP
      END
```

```
      SUBROUTINE FEX (NEQ,T,Y,YDOT)
      IMPLICIT REAL*8(A-H,O-Z)
      COMMON /D/ RK1,RKM1,RK20,RK21,RKM2,RK13,RKHOI,RKW,PH,HCON,
     1RK3,RKM3,RKP4,XTIME,YNNN,YC
      DIMENSION Y(10),YDOT(10),YO(10),XTIME(150),YNNN(150,10)
      YDOT(1)=-RK1*Y(1)+RKM1*Y(2)*Y(3)*HCON
     1+RKP4*HCON*Y(2)
      YDOT(2)=RK1*Y(1)-RKM1*Y(2)*Y(3)*HCON
     1+2./3.*RK20*(Y(3)-YC(6))**2+2./3.*RK21*(Y(3)-YO(6))*YO(6)
     2-2.*RKM2*Y(4)*Y(2)**2*HCON**2
     3-RKP4*HCON*Y(2)
      YDOT(3)=RK1*Y(1)-RKM1*Y(2)*Y(3)*HCON
     1-RK20*(Y(3)-YO(6))**2-RK21*(Y(3)-YO(6))*YO(6)
     2+3.*RKM2*Y(4)*Y(2)**2*HCON**2
      YDOT(4)=1./3.*RK20*(Y(3)-YO(6))**2+1./3.*RK21*(Y(3)-YO(6))*YO(6)
     1-RKM2*Y(4)*Y(2)**2*HCON**2
      YDOT(5)=RK3*Y(1)*Y(2)-RKM3*Y(5)
      RETURN
      END
```

```
      SUBROUTINE JEX(NEQ,T,Y,ML,MU,PD,NRPD)
      IMPLICIT REAL*8(A-H,O-Z)
      COMMON /D/ RK1,RKM1,RK20,RK21,RKM2,RK3,EKHOI,EKW,PH,HCON,
     1RK3,RKM3,RKP4,XTIME,YNNN,YC
      DIMENSION Y(10),PD(NRPD,5),YC(10),XTIME(150),YNNN(150,10)
      PD(1,1)=-RK1
      PD(1,2)=RKM1*Y(3)*HCON
     1+RKP4*HCON
      PD(1,3)=RKM1*Y(2)*HCON
      PD(2,1)=RK1
      PD(2,2)=-RKM1*Y(3)*HCON-4.*RKM2*Y(4)*Y(2)*HCON**2
     1-RKP4*HCON
      PD(2,3)=-RKM1*Y(2)*HCON+4./3.*RK20*(Y(3)-YC(6))+2./3.*RK21*YC(6)
      PD(2,4)=-2.*RKM2*Y(2)**2*HCON**2
      PD(3,1)=RK1
      PD(3,2)=-RKM1*Y(3)*HCON+6.*RKM2*Y(4)*Y(2)*HCON**2
      PD(3,3)=-RKM1*Y(2)*HCON-2.*RK20*(Y(3)-YC(6))-RK21*YC(6)
      PD(3,4)=3.*RKM2*Y(2)**2*HCON**2
      PD(4,2)=-2.*RKM2*Y(4)*Y(2)*HCON**2
      PD(4,3)=2./3.*RK20*(Y(3)-YC(6))+1./3.*RK21*YC(6)
      PD(4,4)=-RKM2*Y(2)**2*HCON**2
      PD(5,1)=RK3*Y(2)
      PD(5,2)=RK3*Y(1)
      PD(5,5)=-RKM3
      RETURN
      END
```

```
      SUBROUTINE KIPLOT(NEXP,NN)
      IMPLICIT REAL*8 (A-H,O-Z)
      INTEGER*4 IBITLE(20)
      REAL*4 XAR(150),YAR(150),XXAR(10),YYAR(10)
      DIMENSION Y(10),YI(10),YN(10),YP(10),YO(10),YNNN(150,10),
     1K1(10),K2(10),K3(10),K4(10),K5(10),P(10),P1(10),IPAK(800),LA
     2B(10),XTIME(150)
      COMMON /D/ EK1,EKM1,EK20,EK21,EKM2,EKI3,EKHCI,EKW,PH,HCON,
     1EK3,EKM3,EKP4,XTIME,YNNN,YC
      DATA INPT,IOUTPT,IPUNCH /5,6,7/
      DATA KCONT /0/,IBEG/-1/
      IF(KCONT.NE.0)GO TO 10
      CALL DSKPLT
      CALL PGNPL(IBEG)
      CALL NOERAS
      CALL NOCHEK
      CALL PAGE(22.,10.5)
      KCONT=KCONT-IBEG
   10 CONTINUE
      CALL PHYSOR (2.5,1.1)
      CALL SCMPLX
      CALL HEIGHT(0.25)
      CALL BASALP ('L/CSTD')
      CALL M1XALP ('STANDARD')
      CALL MX4ALP ('INSTRU','>')
      READ(INPT,2000)(IBITLE(K),K=1,20)
      READ(INPT,1001) XMIN,DEX,XMAX,YMIN,DEY,YMAX
      READ(INPT,1000) XLEG,YLEG,XILEG,XLEN
      LMAX=LINEST(IPAK,800,80)
 2000 FORMAT(20A4)
      CALL TITLE (IBITLE,100,' TIME (() SEC ())$',100,'                $',
     1100,XLEN,7.5)
      CALL MESSAG('MIN$',3,5.29,0.1)
      CALL MESSAG('HR$',2,7.29,0.1)
      CALL MESSAG('DAY$',3,8.60,0.1)
      CALL MESSAG('YR$',2,11.26,0.1)
      CALL ICGLOG (XMIN,DEX,YMIN,DEY)
      YLE=YLEG+1.35
      XLG=XLEG+0.2
      XLE=XLEG+XILEG
      XPN=FLOAT(NEXP)
      YYLEG=YLEG-0.552*XPN+0.7
      CALL BLNK1(XLEG,XLE,YYLEG,YLE,2)
      CALL RESET ('BLNK1')
      XL=5.27
      XDL=9.40
      YL=0.0
      YDL=0.38
      CALL BLNK4(XL,XDL,YL,YDL,0)
      XLL=11.21
      XDLL=11.77
      CALL BLNK2(XLL,XDLL,YL,YDL,0)
      CALL BLNK3(0.0,20.0,0.0,-1.0,0)
```

```
      DO 20 J=1,NEXP
      DO 30 I=1,NN
   11 XAR(I)=YNNN(I,J)
      XAR(I)=XTIME(I)
      IF (J.NE.1) GO TO 30
      XAR(1)=XAR(3)
      XAR(2)=XAR(3)
   30 CONTINUE
      XAR(NN+1)=XIEG+0.1
      XAR(NN+1)=XMIN*10.0**(XAR(NN+1)/DEX)
      YAR(NN+1)=YIEG-0.552*J+1.05
      YAR(NN+1)=YMIN*10.0**(YAR(NN+1)/DEY)
      XXAR(J)=XAR(NN+1)
      YYAR(J)=YAR(NN+1)
      CALL BLNK1(XIG,XLE,YYIEG,YIE,0)
      IF (J.EQ.1) MAR=7
      IF (J.EQ.2) MAR=1
      IF (J.EQ.3) MAR=2
      IF (J.EQ.4) MAR=5
      IF (J.EQ.5) MAR=4
      IF (J.EQ.6) MAR=6
      CALL MARKER(MAR)
      CALL CURVE (XAR,YAR,NN,+1)
      READ(INPT,2000) (IBITLE(K),K=1,20)
      CALL RESET ('BLNK1')
      YSTO=YIEG-0.552*J+0.9
      XSTO=XIEG+0.36
      CALL LINES(IBITLE,IPAK,1)
      CALL LSTORY(IPAK,1,XSTO,YSTO)
      CALL BLNK1(XIG,XLE,YYIEG,YIE,0)
   20 CONTINUE
      CALL RESET('BLNK1')
      DO 50 J=1,NEXP
      XAR(1)=XXAR(J)
      YAR(1)=YYAR(J)
      IF (J.EQ.1) MAR=7
      IF (J.EQ.2) MAR=1
      IF (J.EQ.3) MAR=2
      IF (J.EQ.4) MAR=5
      IF (J.EQ.5) MAR=4
      IF (J.EQ.6) MAR=6
      CALL MARKER(MAR)
      CALL CURVE (XAR,YAR,1,-1)
   50 CONTINUE
      CALL ANGLE(90.)
      CALL MESSAG('CONCENTRATION GATOM/L',21,-1,1.5)
      CALL RESET('ANGLE')
      CALL CORE(LAB,40)
      WRITE(INPT,40)
   40 FORMAT( '(LEGEND) $')
      WRITE(6,2001)LAB
 2001 FORMAT(10A4)
```

```
      XIG=XIG-0.1
      YLP=YLP-0.4
      CALL LINES(LAB,IPAK,1)
      CALL LSTORY(IPAK,1,XLG,YLP)
      CALL RESET('BLNK3')
      CALL RESET('BLNK4')
      CALL RESET('BLNK2')
      YYMIN=YMIN*0.8
      CALL RLVEC(60,YYMIN,60,YMIN,2201)
      CALL RLVEC(3600,YYMIN,3600,YMIN,2201)
      CALL RLVEC(86400,YYMIN,86400,YMIN,2201)
      CALL RLVEC(3.15D07,YYMIN,3.15D07,YMIN,2201)
      CALL FRAME
      CALL ENDPL(1)
 1000 FORMAT(8F10.4)
 1001 FORMAT(E10.0,F10.4,2F10.0,F10.4,E10.0
      RETURN
      END
```

7. REFERENCES

1. J. T. Bell, D. O. Campbell, L. M. Toth, M. H. Lietzke, and D. A. Palmer, *Aqueous Iodine Chemistry in LWR Accidents: Review and Assessment,* ORNL-5824 (1982).
2. M. Eigen and K. Kustin, *J. Am. Chem. Soc.* 84, 1355 (1962).
3. T. R. Thomas, D. T. Pence, and R. A. Hasty, *J. Inorg. Nucl. Chem.* 42, 183 (1980).
4. C. C. Li and C. F. White, *J. Am Chem. Soc.* 65, 335 (1943).
5. D. A. Palmer and M. H. Lietzke, *Radiochim. Acta*, in press.
6. D. A. Palmer, unpublished results.
7. A. F. M. Barton and G. A. Wright, *J. Chem. Soc. (A),* 2096 (1968).
8. J. Sigalla and C. Herbo, *J. Chem. Phys.* 54, 733 (1957).
9. W. Eguchi, M. Adachi, and M. Yoneda, *J. Chem. Eng. Japan,* 6, 389 (1973).
10. W. C. Bray and G. M. J. Mackey, *J. Am. Chem. Soc.* 32, 914 (1910).
11. G. Jones and B. B. Kaplan, *J. Am. Chem. Soc.* 50, 1845 (1928).
12. A. D. Awtey and R. E. Connick, *J. Am. Chem. Soc.* 73, 1342 (1951).
13. M. Davies and E. Gwynne, *J. Am. Chem. Soc.* 74, 2748 (1952).
14. J. D. Burger and H. A. Liebhafsky, *Anal. Chem.* 54, 600 (1973).
15. Y.-t. Chia, Ph.D. thesis, UCRLA311, University of California, Berkeley (1958).
16. W. L. Marshall and E. U. Franck, p. 506 in *Water and Steam,* ed. by J. Straub and K. Scheffler, Pergamon Press, New York, 1980.
17. N. E. Dorsey, p. 583 in *Properties of Ordinary Water Substance in All Its Phases,* Reinhold, New York, 1940.
18. C. M. Kelley and H. V. Tartar, *J. Am. Chem. Soc.* 78, 5752 (1956).
19. H. Margenau and G. M. Murphy, *The Mathematics of Physics and Chemistry*, Van Nostrand, New York, 1956.
20. L. F. Shampine and C. W. Gear, *Soc. Ind. Appl. Math. Rev.* 21, 1 (1979).
21. A. E. J. Eggleton, *A Theoretical Examination of Iodine-Water Partition Coefficients*, AERE-R-4887 (1967).
22. M. J. Kabat, "Chemical Behavior of Radioiodine Under Loss of Coolant Accident Conditions," Proc. 16th DOE Nuclear Air Cleaning Conf. (1980).

NUREG/CR-2900
ORNL-5876
Dist. Category R3

INTERNAL DISTRIBUTION

1. C. F. Baes
2. C. E. Bamberger
3-7. J. T. Bell
8. W. D. Burch
9. D. O. Campbell
10. R. W. Glass
11. H. W. Godbee
12. J. Halperin
13. S. A. Hodge
14. O. L. Keller
15. T. S. Kress
16-20. M. H. Lietzke
21. T. B. Lindemer
22. A. L. Lotts
23. A. P. Malinauskas
24. R. E. Mesmer
25. R. E. Meyer
26. G. D. O'Kelley
27. M. F. Osborne
28-32. D. A. Palmer
33. D. J. Pruett
34. F. M. Scheitlin
35. J. H. Shaffer
36. O. K. Tallent
37. L. M. Toth
38. J. R. Travis
39. S. K. Whatley
40. C. F. Weber
41. C. C. Webster
42. R. P. Wichner
43. R. G. Wymer
44. Laboratory Records
45. Laboratory Records, ORNL RC
46. ORNL Patent Section
47. Central Research Library
48. DRS-Y-12 Library

EXTERNAL DISTRIBUTION

49. Office of Assistant Manager for Energy Research and Development, DOE-ORO, P. O. Box E, Oak Ridge, TN 37830
50-51. Director, Division of Reactor Safety Research, Nuclear Regulatory Commission, Washington, D.C. 20555
52-53. Technical Information Center, DOE, Oak Ridge, TN 37830
54-373. Given Distribution as shown in Category R3 (NTIS-10)

☆U.S. GOVERNMENT PRINTING OFFICE: 1982-546-067/170